Investigating the Impacts of Adverse Road-Weather Conditions on Saturation Headway

By

RYUTARO HIROSE

A Thesis submitted to the Faculty of Graduate Studies of
The University of Manitoba
in partial fulfilment of the requirements of the degree of

MASTER OF SCIENCE

Department of Civil Engineering
University of Manitoba
Winnipeg, Manitoba

Abstract

Adverse road-weather (RW) conditions may deteriorate traffic operations and safety at intersections due to reduced capacity, frequent collisions, and increased traffic emissions. Weather responsive traffic management (WRTM) can potentially lessen the negative impact of adverse RW conditions. Yet, saturation flow rate (SFR) is a major input for any WRTM that is affected by RW conditions and traffic composition. Few studies investigated the combined effect of adverse RW conditions and heavy vehicle (HV) ratios on the operation of signalized intersections. Additionally, the classic method for measuring SFR estimates the mean of observed flow rates starting from a critical vehicle (CV), i.e., 5^{th} vehicle in the queue per cycle which has several shortcomings including: (1) not considering the probabilistic nature of SFR, (2) ignoring the unsaturated vehicles in the queue i.e., vehicles preceding the CV, and (3) using a particular CV threshold regardless of RW conditions. This thesis investigates saturation headway variations considering RW conditions and HV ratios using the data collected at two busy signalized intersections in Winnipeg, Canada. Regression analysis was used to analyze saturation headways and passenger car equivalent (PCE) factors considering RW conditions. Further, a novel methodology is proposed to model SFR variations using survival analysis that was implemented to explore the stochastic characteristics of SFR considering different CV settings and RW conditions. The findings confirmed that adverse RW conditions can increase the saturation headway significantly e.g., by up to 38.7% for snowy RW conditions. Estimated PCE values under each RW classification and the regression models implied that HVs are less susceptible to adverse RW conditions in terms of their impact on saturation headway. The results from the proposed survival analysis method indicated that adverse RW conditions tend to move the CV position forward to the head of the queue. The findings of this thesis provide a practical method for estimation of SFR at signalized intersections under different adverse RW conditions and contribute to establishment of WRTM strategies to improve the safety and operation of signalized intersections in winter.

(331/350 words)

Contributions of Authors

The contents in the second and third chapters of this thesis reproduces the material from prepared research articles. The title of the articles, their status as of the date of submission of the thesis, and authors' contributions are as follows:

1. The article titled *"Investigating Combined Impact of Adverse Road-Weather Conditions and Heavy Vehicles on Saturation Headway"* has been published in Transportation Research Record in 2022. The contents are presented in Chapter 2.

   Authors' contributions to the paper:

   - Study conception and design: R. Hirose, B. Mehran
   - Data collection: R. Hirose
   - Analysis and interpretation of results: R. Hirose, B.Mehran, A. Pani
   - Draft manuscript preparation: R. Hirose, B. Mehran, A. Pani

2. The article titled *"Implementing Survival Analysis to Capture Stochastic Characteristics of Saturation Flow Rate Considering the Impacts of Adverse Road-weather Conditions"* has been submitted to Transportation Research Record and is currently under review. The content is presented in Chapter 3.

   Authors' contributions to the paper:

   - Study conception and design: R. Hirose, B. Mehran
   - Data collection: R. Hirose
   - Analysis and interpretation of results: R. Hirose, B. Mehran, A. Pani, R. Omrani, P. Sahu
   - Draft manuscript preparation: R. Hirose, B. Mehran, A. Pani, R. Omrani, P. Sahu

Acknowledgement

I would like to express my gratitude to all the people who have supported me in completing this thesis. Foremost, I am genuinely grateful to my supervisor Dr. Babak Mehran for providing me with this opportunity to pursue MSc in Canada. His broad knowledge, clear explanations, tolerant guidance, and financial support contributed to my research work. His professional attitude toward research and other people exemplifies a strong leadership for me to achieve in the future.

My profound appreciation goes to Dr. Agnivesh Pani. Without his help, it would not be possible to finish this thesis. Out of his busy schedule, he spared much time for the revisions of the papers and discussions on the analysis. He provided me with plenty of insightful suggestions to refine my research and helpful modifications to draft scientific papers.

My fellow friends in our research group have enlightened me about research work, welcomed me to adjust to my life as an international student, and supported me by sharing their experiences. While we all had to go through the COVID-19 pandemic and experience remote companionship for the most part of my studies at the University of Manitoba, it was sincerely fortunate that I could join this research group. Moreover, I also thank my advisory and examining committee members: Dr. Reza Omrani, Dr. Prasanta Sahu and Dr. Jonathan Regehr for providing thought-provoking ideas and valuable suggestions to improve my research. Besides, I extend my appreciations to the City of Winnipeg for providing the video data and the Natural Sciences and Engineering Research Council of Canada (NSERC) for funding my research program.

I also convey my special thanks to Prof. Hideki Nakamura and Dr. Yuji Kakimoto, who supervised my bachelor's research in Japan. They affectionately cared about my study and motivated me to do my graduate studies in Canada.

Lastly, I owe a substantial debt to my parents, Kazuya and Yoshie, and my sister Kasumi. They have encouraged me by dedicating financial and mental support throughout my life. Thank you for all your help.

Table of Contents

List of Tables

List of Figures

List of Abbreviations

This thesis uses some acronyms for simplification. The following list is a description of the important abbreviations and the sections where they are specifically defined or explained in this thesis.

Acronym	Description	Section
WRTM	Weather Responsive Traffic Management	1.1.2
SFR	Saturation Flow Rate	2.1
HV, PC	Heavy Vehicle, Passenger Car	2.3.2
RW	Road-Weather	2.3.3
PCE	Passenger Car Equivalent	23
CV	Critical Vehicle	3.4.1
HCM	Highway Capacity Manual	see References
CCG	Canadian Capacity Guide 3rd edition (ITE 2007)	see References
FHWA	Federal Highway Administration	see References

1 INTRODUCTION

1.1 Background

In designing intersections, traffic engineers aim to optimize traffic efficiency, safety, environmental burden, geometrical restriction, and cost. Weather conditions affect driving attitudes and vehicle performance, rendering the optimal traffic planning challenging. Especially adverse road-weather (RW) conditions, e.g., snowy, icy, rainy, and slushy, have been recognized as a significant cause of severe traffic congestion, worsened road safety performance, and even increased environmental burden (Agbolosu-Amison et al., 2004). Previous research has shown that inclement weather impacts the traffic parameters and proposed how to incorporate the weather-related effect into the system control (Agbolosu-Amison et al., 2004). The following three sections review that prior research on, firstly, the impact of adverse weather on traffic parameters, secondly, state-of-the-art traffic management technology tailored for adverse weather, and thirdly, current well-known signal timing design approaches.

1.1.1 Impact of Adverse Weather on Traffic

For effect on traffic mobility, the *Canadian Capacity Guide* (CCG) warns that extreme winter conditions with heavy snowfall, blizzard, freezing rain, or a slippery pavement condition may create extremely long headways (ITE, 2007). To address this fact, CCG recommends determining applicable saturation flow rate (SFR) values to local weather events (Teply et al., 1983). The guide, however, does not specify any pragmatic approach for integrating the weather impact into traffic management. Not many, but some studies have been conducted in the past on the impact of severe weather on traffic-related parameters.

For instance, free-flow speed, an essential index for the highway LOS assessment, is known to be vulnerable to the driving environment. In this regard, Ibrahim and Hall (2004) studied the speed-flow-occupancy relationship in Ontario, Canada, and performed a regression analysis. The results exhibited that heavy rain and snow caused a drop in free-flow speeds by up to 10 km/h and 50 km/h, respectively. The study also observed a sizable reduction in maximum flows by 10 to 48 % due to heavy rain or snow, while light precipitation showed a negligible effect. Yasanthi and Mehran (2020) examined free-flow speeds on a highway in Alberta, Canada, using Road-Weather-Information-System and Weigh-in-Motion station data. Their study specifies the reduction in free-flow speed for each lane and vehicle type, as shown in Table 1.1. Based on the results that snowy and icy RW conditions decrease free-flow speed, the authors highlighted that frequent snow and ice removal would mitigate the weather-related delays and improve safety performance without reducing desired speeds.

Table 1.1: Reduction Rate in Free Flow Speeds (Yasanthi and Mehran, 2020)

	Present Study		Kyte et al. (2000)	HCM (2016)
	Light Vehicles	Heavy Vehicles		
Slight Snow	−0.2%	−1.7%	−3.2%	−8%
Moderate Snow	−3.4%	0.1%	−11.6%	–
Heavy Snow	−0.8%	−1.3%	−20.1%	−41.6%
Wet Pavement	−0.3%	0.3%	−5.3%	–
Snow/Icy Pavement	−2.2%	−2.6%	−10.5%	–

Note: [1] $Speedreductionfactor = \frac{FFSinclearRW - FFSinadverseRW}{FFSinclearRW} \times 100.$

In addition, Sadek and Agbolosu-Amison (2004) assessed start-up lost time and SFR (Saturation Flow Rate) at intersections in northern New England. Table 1.2 summarizes the mean values of obtained start-up lost time, SFR and its reduction percentage compared to dry RW conditions. It can be clearly interpreted that severe slushy and snowy RW conditions have a considerable negative impact on SFR.

Table 1.2: Summary of Values Obtained for Startup Lost Time and Saturation Headways (Sadek et al., 2004)

Road Condition	Startup Lost Time		Saturation Headway (Saturation Flow Rate) [1]		% Reduction in Saturation Flow Rate	
	EB	WB	EB	WB	EB	WB
1. Dry	2.20	1.84	2.24 (1607)	2.04 (1766)	0%	0%
2. Wet	2.42	1.98	2.31 (1558)	2.08 (1734)	3%	2%
3. Wet and Snowy	2.18	2.28	2.42 (1490)	2.13 (1691)	7%	4%
4. Wet and Slushy	1.29	2.00	2.41 (1491)	2.39 (1505)	7%	15%
5. Slushy in WP	---[2]	1.90	---[2]	2.58 (1396)	---[2]	21%
6. Snowy and Sticky	3.04	2.20	2.67 (1348)	2.44 (1475)	16%	16%

As for road safety, according to a report by Manitoba Public Insurance (MPI, 2020), there were 70,081 collisions reported in Manitoba, Canada. Any crashes related to injury or property damage only (PDO) happened more frequently in the winter snow falling season. However, the fatality was more notable in summer, as shown in Figure 1.1. In winter, conservative driving behaviour may result in these fewer fatalities but induces difficulties in steering the wheel and a

considerable increase in minor collisions. Figure 1.2 provided by MPI also shows the collision rate by RW, which indicates that 63 % of crashes happen under dry RW conditions. Despite the careful driving attitude, over 25 % of collisions occurred under icy or snowy RW conditions.

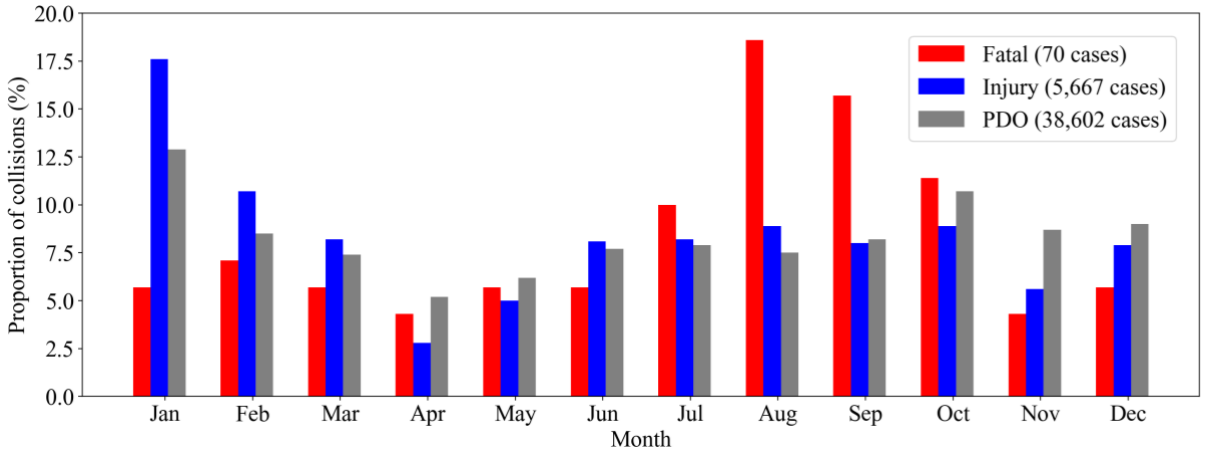

Figure 1.1: Collisions by Month of Occurrence and Collision Severity in Manitoba 2020 (MPI, 2020)

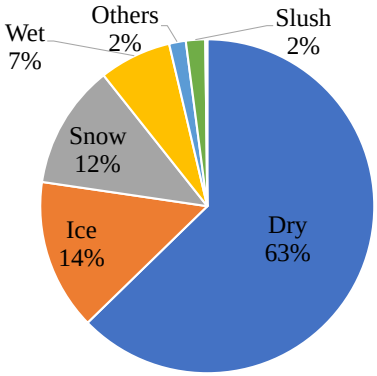

Figure 1.2: The Rate of Reported Collisions by RW Conditions in Manitoba 2020 (MPI, 2020)

In a case study in New England, Agbolosu-Amison et al. (2004) shed light on the negative environmental implications of winter driving. The study found an increase in fuel consumption by 3 % on the snowy road due to the considerable control delay, frequent stops, and reduced speed. In another attempt in greater Mumbai, India, Soni et al. (2019) confirmed the increasing trend of fuel consumption with rainfall intensities. They also specified that travel time under very heavy rainfall (64.5 mm/day to 124.4 mm/day) was up to 136 % longer than that of no precipitation.

1.1.2 Importance of Weather Responsive Traffic Management

To achieve safe, reliable, and efficient traffic flows simultaneously, the Federal Highway Administration (FHWA) recommends implementing Weather Responsive Traffic Management (WRTM) scheme, which effectively deals with traffic flow during inclement weather (FHWA, n.d.). Pisano and Goodwin (2004) categorized WRTM into three strategies: Advisory, Control and Treatment:

- Advisory strategies provide public travellers with timely traffic and weather information to notify ongoing traffic and weather states. For informed individual decision, many jurisdictions deploy the advisory WRTM. For this strategy, timelier and more accurate alerts should be sent for better communication between public travellers and traffic agencies.
- Control strategies take advantage of the roadway information to allow or impede traffic flows. The strategies encompass the adjusted signal timing, speed management, and traffic monitoring so that traffic planners can deal with traffic congestions and unsafe events under adverse weather as needed.
- Treatment strategies aim to mitigate the negative weather impact by removing accumulated snow, ice and rain or restoring damaged infrastructures. These operations will directly contribute to maintaining the traffic conditions as ideal.

In recent years, the advent of high-speed data transmission, Connected Autonomous Vehicles and related technologies have facilitated the development of real-time data acquisition environments as the first stage of WRTM. In this background, FHWA (2017) reported that over 20 States in the U.S. are establishing the communication mechanism with sensors and software tools on roads as a WRTM initiative. The Texas A&M Transportation Institute research team deployed WRTM strategies on the corridors in Texas and evaluated the effect on traffic performance (Balke et al., 2017). The study concluded that WRTM reduced the delay, the number of stops, and the queue length, but the effect would be limited to the places where high volume exists and vehicles drive at high speed. From operational point of view, it is expected that WRTM

would be an efficient control scheme to alleviate the negative impact of weather on traffic flows at some specific locations.

Sadek et al. (2004) conducted a comprehensive simulation of "special" signal timing using four simulation platforms: TRANSYT-7F (McTrans, 2021), SYNCHRO (Trafficware, 2011), CORSIM (FHWA, n.d.), and SimTraffic (Trafficware, 2011). The signal timings for inclement weather, i.e., Dry, Wet, Wet and Snowy, Wet and Slushy, Slushy in Wheel paths, and Snowy and Sticky were programmed using the average percentage of reduction in SFR and free-flow speed. Using the uniquely-adjusted signal timing, operational benefits appeared in the delay, travel time, stops and fuel consumption. This study showed consistent output with the aforementioned study in Texas, as the benefits seemed to be more significant for segments with higher traffic and longer distance between consecutive intersections.

1.1.3 Introduction to the Current Signal Timing Determination

Operation of signalized intersections where complex movements of vehicles and pedestrians are involved is essential for a better transportation network. About 25,000 signals are placed across Canada, and microprocessor-based controllers and traffic detection devices are introduced to most signalized intersections (NTOC, 2012). In designing a signalized intersection, signal timing is its core to give balanced priorities to drivers, pedestrians, cyclists, and public transits. One primary control tactic of WRTM is also to adjust traffic signal timing in response to the surrounding weather conditions at short time intervals as possible.

According to CCG, isolated signal timing is planned in three steps: ***Step1.*** *Gather necessary information on the geometry and traffic volumes;* ***Step2.*** *Estimate cycle length;* ***Step3.*** *Determine phase splits.* More detailed procedures are described below:

Step1. *Gather necessary information on the geometry and traffic volumes*

The first step of implementing a traffic signal to an intersection or evaluating a signalized intersection is to gather relevant information in the vicinity of the intersection to project the traffic demand. The required information is the geometry of the intersection, estimated

traffic volume and SFR, and the traffic conditions upstream and downstream of the intersection. Out of this necessary information, SFR is relatively difficult to measure and requires extensive data analysis because SFR can be observed when the transition state between uncongested and congested occurs.

When directly measuring SFR from traffic records at intersections, the *Highway Capacity Manual 6th* (HCM) suggests periodically taking an average of flow rates from the fifth vehicle until the last vehicle in the queue waiting for the green signal (TRB, 2016). This method is oriented to the idea that the flow rates associated with the first four vehicles in a queue are unsaturated due to start-up lost time and should be ignored from the SFR calculation. The "fifth vehicle" as a threshold derived from empirical studies often preferred in the existing research to examine SFR for its simplicity. This field measurement is powerful to see the intrinsic SFR to a specific intersection but requires extensive and careful data collection.

In this difficulty, when indirectly estimating SFR, HCM recommends a multiplicative model to adjust a base SFR value with multiple geometric and traffic condition factors shown in Equation (1.1). Base SFR is the expected average flow rate for through traffic lane assuming the most favorable traffic conditions and environment. The suggested default value in HCM is 1,900 (pc/h/lane) for the place with over 250,000 population.

$$q_{s(adj)} = q_{s(base)} \cdot f_w f_{HVg} f_p f_{bb} f_a f_{LU} f_{LT} f_{RT} f_{Lpb} f_{Rpb} f_{wz} f_{ms} f_{sp} \quad (1.1)$$

where

$q_{s(adj)}$ = adjusted SFR (veh/h)

$q_{s(base)}$ = base SFR (veh/h)

f = adjustment factor for

w = lane width,

HVg = heavy vehicles and grade,

p = existence of parking lane and parking activity,

bb = blocking effect of local buses that stop within intersection area,

a = area type,

LU = lane utilization,

LT = left-turn vehicle presence,

RT = right-turn vehicle presence,

Lpb = pedestrian bicycle adjustment for left-turn group,

Rpb = pedestrian-bicycle adjustment for right-turn group,

wz = work zone presence at the intersection,

ms = downstream lane blockage, and

sp = sustained spillback

Step2. *Estimate cycle length*

Based on the collected data, signal phasing and estimated lost time will be determined accordingly. HCM shows that assuming 2 (s) as a start-up lost time per phase is appropriate. Then, the cycle length c is determined from some given inputs and estimated traffic state. The cycle length ranges typically from 60 and 140 (s). While too short cycle length does not carry the coming traffic adequately, excessive cycle length is also undesirable. That is not only because it increases delays, but also because it increases the waiting time for drivers and pedestrians, which can be a culprit of a psychological impact and induce jaywalking. Therefore, a maximum cycle length of around 120 (s) is also considered realistic with some exceptional jurisdictions.

A condition that traffic demand should be less than the SFR should be at least satisfied in determining an appropriate cycle length. Under this assumption, minimum cycle length will be derived in Equation (1.2).

$$c_{\min} = \frac{L}{1-\lambda} \tag{1.2}$$

where

C_{min} = minimum cycle length (s)

L = intersection lost time (s)

λ = intersection flow ratio (ratio of traffic demand to SFR)

Given that traffic flow rates always have fluctuation, operating at capacity level with minimum cycle length is not proper. For this fact, Webster and Cobbe (1966) performed a simulation if traffic flows follow Poisson distribution and formulated the optimum cycle length to accommodate the arrival flows and minimize the total intersection delays in Equation (1.3).

$$c_{opt} = \frac{1.5L + 5}{1 - \lambda} \tag{1.3}$$

where

C_{opt} = optimum cycle length (s)

L = intersection lost time (s)

λ = intersection flow ratio (ratio of traffic demand to SFR)

Step3. *Determine phase splits*

Then, the cycle length c will be allocated to the green, red, and amber phase mostly by iterative computing. This step involves the purpose of building the intersection. To meet the requirements, phase splits will be set to balance flow ratio, minimize vehicle's total delay, minimize specific approach's delay, or minimize pedestrian's delay etc.

Evaluating the final signalized intersection's capability, traffic lane capacity C, which is the maximum number of vehicles that can pass a certain point on a lane in each unit time is estimated in Equation (1.4).

$$C = \frac{g_e}{c} \cdot q_s \tag{1.4}$$

where

C = traffic lane capacity (veh/h)

g_e = effective green time (s)

c = cycle length (s)

q_s = SFR (veh/h)

1.2 Motivations of the Thesis

As seen from the reviews above, some experts contended the negative impact of weather conditions on the driving environment. Additionally, this world experiences growing demand for passenger cars and commercial vehicles as Figure 1.3 illustrates (MPI, 2020). As freight traffic also becomes demanding these days, it is anticipated that efficient traffic operation with integrating the impact of heavy vehicles (HVs) under adverse RW conditions would be more necessary where the HV ratio is considerable. Moreover, since SFR is predominant for determining signal split and capacity, the precise measurement and estimation of SFR are vital for the cooperative signal design and the accurate evaluation of intersection control especially associated with WRTM. To accomplish the reliable and flexible WRTM, it is now required to establish simple and practical approach to accurately measure the intersection's performance under different RW conditions.

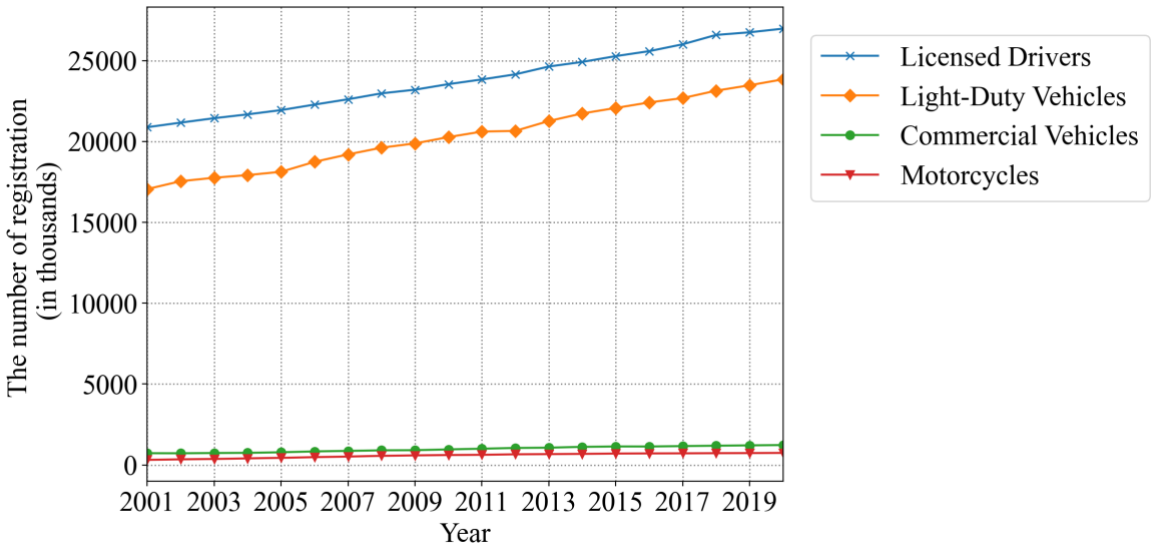

Figure 1.3: The Number of Registrations of Drivers and Vehicles (MPI, 2020)

1.3 Problem Statement

Some scholars have perceived the necessity of considering the weather's impact on traffic management and insisted that investigations on the effect of weather on traffic parameters should be accelerated to support traffic manager's decision making and facilitate WRTM in the cold regions (Sadek et al., 2004; Pisano and Goodwin, 2004; Lu et al., 2019). CCG (2007) also

recommends flexibly determining the applicable SFR values to the local weather conditions to address the expected climate-related incidents. However, most manuals are still based on the results under ideal weather conditions, and no practical approach to reflect weather interference on its management is provided in the guidelines (ITE, 2007; TRB, 2016).

Moreover, it is crucial to reconsider the conventional approach to measure better and localized SFR in this transition era to the up-to-the-minute adjusted traffic systems. The deterministic SFR value as an average value in the HCM method smothers its stochasticity and ignores information of unsaturated flow rates. In addition, the empirical belief that start-up lost time dissipates from a Critical Vehicle (CV), typically the "5th vehicle", and flow rates become mostly steady as SFR has not been statistically tested. The queuing threshold vehicle might be defined at different positions among different RW conditions.

1.4 Objectives

The common goal throughout this thesis is to strengthen the necessity of WRTM and open windows for more flexible intelligent WRTM by examining the effect of adverse RW conditions on the saturated traffic at signalized intersections. This goal is achieved through the objectives in the subsequent two chapters and listed as follows:

Primary objectives:

Chapter 2 focuses more on the statistical clarification of the impact of adverse RW conditions on saturation headways under varying HV ratios. This study targets two signalized intersections, both of which carry around 50,000 (veh/day) for both directions combined in Winnipeg, Canada (City of Winnipeg, 2019). Winnipeg experiences snow falling for about half a year, as shown in Figure 1.4 (Historical Climate data, 2021). The detailed objectives are:

- To statistically show the variation of saturation headways due to adverse RW conditions;
- To show the HV's interference on the impact;
- To model saturation headways with respect to adverse RW conditions and HV ratio.

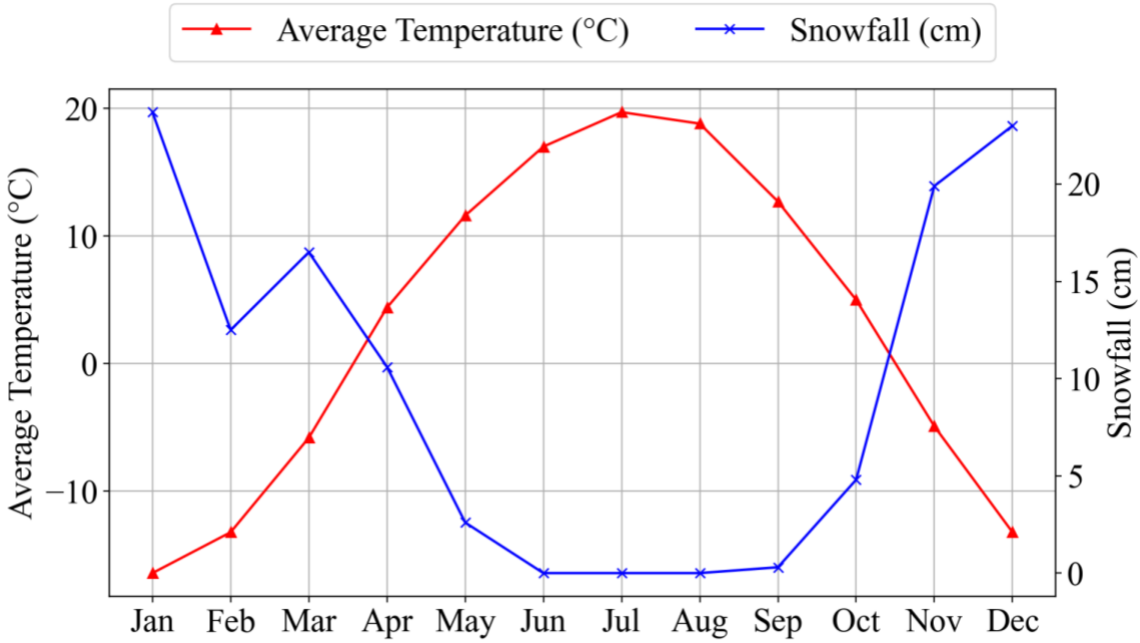

Figure 1.4: Average Snowfall and Temperature from 1981 to 2010 in Winnipeg (Historical Climate Data, 2021)

Secondary objectives:

Chapter 3 focuses more on pointing out the pitfalls of the conventional SFR concept and its calculation approach and offering a countermeasure. The detailed objectives are:

- To suggest a stochastic concept of SFR
- To show probabilistic SFR distributions under adverse RW conditions;
- To propose statistical approaches for flexibly finding an optimal CV;
- To justify using different CVs under adverse RW conditions.

1.5 Structure of the Thesis

This thesis is structured as a grouped manuscript or sandwich-style thesis. The following two chapters are self-contained research papers, consisting of owning its abstract, introduction, literature review, methodology, results and discussion, and conclusion. Please be noted that some parts are slightly modified from their original for the smooth integration in this thesis.

- Chapter 2 is a research paper that describes the combined impact of adverse road weather and heavy vehicles on saturation headways to address the primary objectives.
- Chapter 3 is another research paper that presents the stochastic concept of SFR to address the secondary objectives.
- Chapter 4 concludes the entire thesis by recapping the contributions of each research paper to the actual traffic management and analysis and offers its potential for future research extension.

2 INVESTIGATING COMBINED IMPACT OF ADVERSE ROAD-WEATHER CONDITIONS AND HEAVY VEHICLES ON SATURATION HEADWAY

This chapter begins with the analysis of saturation headways under several different RW conditions and different HV ratios. The definition of "Saturated" is based on the commonly-used HCM (2016) method, in this chapter. It aims to clarify the variation of saturation headway due to the snowy or icy pavement conditions and its combined impact with HV existence in the traffic stream. The analysis of this chapter, especially the modelled saturation headways, ultimately contributes to the adjustment of signal timing depending on the weather conditions and HV ratio to achieve an increase in the capacity of a signalized intersection. Besides, it also helps us in conducting a more accurate simulation of traffic flows.

The material in this chapter is published in Transportation Research Record (Hirose et al., 2022), and reprinted with permission of the publisher and co-authors Agnivesh Pani and Babak Mehran. The chapter is self-contained with its own abstract, introduction and conclusion; acknowledgements are provided in the preface of the thesis and references are provided at the end of the thesis. The thesis author conducted the analysis, interpreted the results, and prepared the manuscript.

2.1 Abstract

Adverse road-weather (RW) conditions make driving behaviour more conservative and the headway during saturated conditions longer, leading to a significant reduction in the capacity of signalized intersections. Past studies indicate that the degree of the influence of adverse RW conditions on intersection performance changes by heavy vehicle (HV) ratio in traffic flow. However, little is known regarding the combined impacts of adverse RW conditions and HV ratio on saturation headway and how they can be considered in the planning of signalized intersections in areas with long winter. To fulfill this research gap, in this study the saturation headway data for over 2,000 signal cycles were extracted from video recordings at two signalized intersections in Winnipeg, Canada. The combined impacts of adverse RW conditions and HV ratios are statistically investigated in the paper with due focus given to saturation headway distributions and

models. To account for differences in vehicle types, passenger car equivalent and headway distributions are evaluated under different RW conditions. The analysis findings suggest that the saturation headways increased by up to 38.7% due to adverse RW conditions. The multiple regression analyses incorporating HV ratios quantify the relationship between saturation headway and various sets of explanatory variables covering adverse RW conditions and roadway geometric factors. The model estimation results reveal that the heavy vehicles are less sensitive to RW conditions than passenger vehicles. Overall, the study findings will help in designing signalized intersections under adverse RW conditions with various HV ratios.

Keywords: Saturation headway; Adverse weather; Heavy vehicle ratio; Signalized Intersections; Intersection Capacity

2.2 Introduction

In the planning and design of signalized intersections, saturation flow rate (SFR), which is defined as “the rate at which vehicles that have been waiting in a queue during the red interval cross the stop line of a signalized intersection approach lane during the green interval” (ITE, 2007), is essential for calculating intersection capacity. SFR for a specific lane (or lane group) is estimated considering base saturation flow rate (veh/h), i.e., the inverse of saturation headway (s), intersection geometry (e.g., lane width and grade), traffic flow characteristics (e.g., right/left turn volume and traffic composition), and lane utilization pattern. The calculation methods for SFR in most intersection planning manuals are based on traffic analysis results under the assumption of ideal RW conditions. The application of this approach to winter weather conditions has been questioned since it is hypothesized that SFR varies greatly depending on road surface and weather conditions (ITE, 2007). This is a significant concern for North American regions with extreme weather conditions in winter such as most northern US states and the Canadian provinces. For example, winter season with extreme cold and snowy conditions can last for about half a year in the Candian prairie provinces (i.e., Manitoba, Saskatchewan and Alberta). It is well documented that poor visibility due to snowfall, and icy roads has negative impact on traffic operations and safety (Teply et al, 1977, 1983). Thus, the importance of considering RW conditions in signal timing design and operational planning of signalized intersections is well-recognized. The

Canadian Capacity Guide (2007) for Signalized Intersections advises determining applicable SFR values depending on RW conditions to assess potential difficulties, which rarely arise under typical dry weather conditions. On the other hand, it is assumed that the degree of the influence of RW conditions on SFR changes by HV ratio in traffic flow and differs between passenger cars (PCs) and HVs. However, the impacts of HVs on saturation headways observed at signalized intersections under adverse RW conditions are still not fully quantified in the academic literature. Furthermore, Passenger Car Equivalent (PCE) for HVs, which is the number of passenger cars having equivalent impact on traffic stream as an HV, is generally adopted as a constant value of 2.0 regardless of RW conditions (Botha et al. 1992).

To address this discernible research gap, this study analyzes saturation headway variations under adverse RW conditions and different HV ratios using video recordings at two signalized intersections in Winnipeg, Manitoba. Observed saturation headways are classified based on RW conditions and vehicle types. Derived PCE values under different adverse RW conditions are compared with *Highway Capacity Manual* (TRB, 2016) value and the relationship between saturation headway and HV ratios are examined under different RW conditions. Finally, different saturation headway models are developed to quantify the compound impact of RW conditions and HV proportions. The study findings are expected to provide a better insight into factors influencing the capacity of signalized intersections in cold regions in North America and elsewhere in the world with comparable RW conditions, especially where the impacts of adverse RW conditions and HV traffic are combined.

The remainder of the paper is structured as follows: first, we provide an overview of the study background with key focus on literature related to the impact of adverse weather conditions on traffic parameters. The study methods including the data collection are presented in subsequent section followed by discussions on implications of RW conditions and HV traffic, and their varying degree of influence. The next section describes saturation headway distributions analysis and modelling, and the last section concludes the paper.

2.1 Literature Review

Several studies investigated the implications of adverse RW conditions on intersection operations including the impacts on traffic parameters such as saturation flow rates, start-up delay and free-flow speed. Perrin et al. (2001) estimated the reduction in the saturation flow rate ranged from 6 % (rain) to 20% (snowy and sticking), speed was reduced by 30% at most and start-up lost time increased by 23% in Salt Lake City, Utah. In an analysis in Waterloo, Ontario, Lu et al. (2019) quantified weather impacts on signal design-related traffic parameters analyzing video recordings of a signalized intersection. They found saturation flow rate decreased by 17% on slushy roads and 25% on the snowy road compared to ideal RW conditions. Further in their study, they observed that free-flow speed declined as much as 23% on the snowy road, while start-up delay showed little change. In New England, Agbolosu-Amison et al. (2004) also confirmed that inclement RW conditions caused a reduction in saturation headways in the range of 2% to 21% combined with rain intensity. Chodur et al. (2011) focused more on comprehensive analysis of saturation flow rate in Polish intersections. In their research, it was found that adverse weather conditions produced a shorter initial interval where start-up lost time appeared and a shorter middle interval i.e., the interval during which saturation headway is stable in a cycle. Prevedouros et al. (2005) compared wet road conditions with the usual dry condition and reported 4.7% reduction in the capacity of arterial streets in Honolulu, the U.S. Their linear regression headway model suggested that observed headways are 4% longer in rainy or wet conditions. Further, they confirmed that wet conditions deteriorated Level of Service by one level in four out of five intersections surveyed in their study. For HV' implications under different RW conditions, Asamer et al. (2011) investigated 2 hours of video recording with 100 signal cycles in Vienna, Austria and measured PCU values under dry, wet and snowy conditions. However, they concluded that the larger PCU values with higher standard deviations observed under dry conditions resulted from lacking sufficient sample size. In another research effort in Asia, Alhassan et al. (2012) found that PCE values decreased with an increase in rainfall intensity in a highway section in Malaysia.

In addition, the need for weather-responsive traffic signal management was highlighted in past research. Lu et al. (2019) implemented an adjusted signal timing in response to weather-related delays in Synchro and VISSIM traffic microsimulation software, and measured intersection

delay in simulation environment for two scenarios i.e., an isolated signalized intersection and a coordinated corridor with four signalized intersections. They showed that, their proposed weather-adjusted signal timing plan could reduce the delay by up to 19.2% when traffic demand was relatively high or medium in both scenarios. In addition to reduced delay, Agbolosu-Amison et al. (2004) found that their proposed weather-adjusted signal timing plan could reduce the number of stops and fuel consumption by up to 8.3% and 4.5%, respectively.

Review of existing studies confirms the need for further research to analyze the impact of weather-related variations in traffic performance and operation of signalized intersections in winter. There are limited studies focusing on the impact of snow and ice as most existing studies only consider rain and wet road surface conditions. In addition, the combined impact of RW conditions and traffic composition i.e., HV ratio has not been studied adequately. Yet, there is concensus that HVs noticeably influence traffic parameters as a result of their larger vehicle size and limited maneouverability (HCM, 2016; Alhassan et al., 2012).

2.3 Data and Methods

2.3.1 Location and Overview of the Study Intersections

This analysis focuses on two signalized intersections in Winnipeg, Canada: Century St & Ness Ave (Century) and Dugald Rd & Lagimodiere Blvd (Dugald) shown in Figure 2.1. The target intersections have lane width of 12 ft or 13 ft, and the southbound approaches are assigned for exclusive through, shared through with right turn, and exclusive left-turn traffic. Traffic signal operation at both intersections are similar as shown in the phase diagrams in Figure 2.2. At the beginning of the green phase, the traffic stream was primarily saturated with queues during most of the observation periods. Both intersections carry significant volumes of PCs and HVs. In particular, on the southbound center lane next to the shoulder lane at Century, 26% of all observed cycles contained at least one HV.

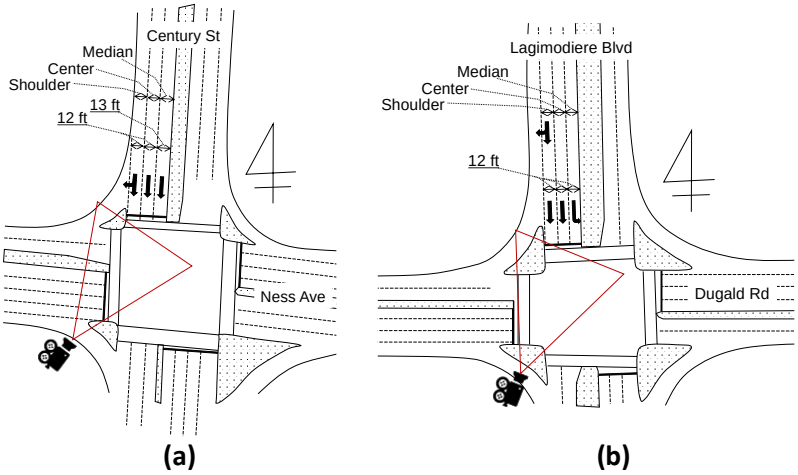

Figure 2.1: Sketches of Intersections (a) Century and (b) Dugald

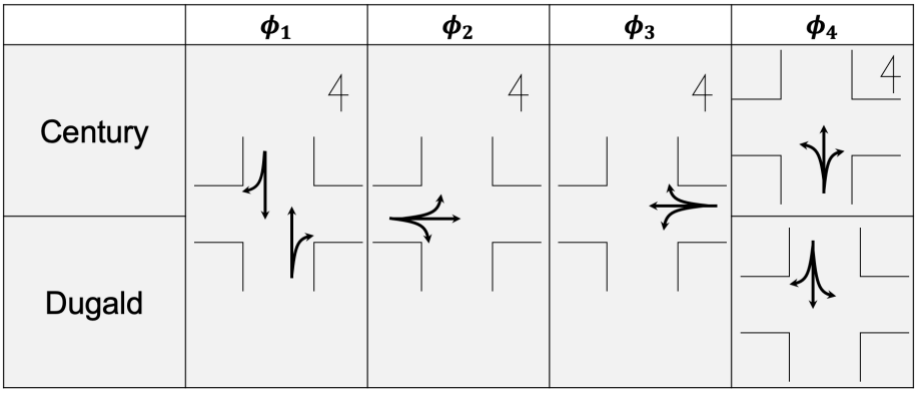

Figure 2.2: Four Phases Signal Operations at Century and Dugal

2.3.2 Data Collection for Saturation Headway

Headway data was extracted from video recordings captured by overhead cameras fixed ahead of the direction of flows at the target intersections. A total of 71 hours of video footage was taken in the morning (7:30-9:30) and afternoon (15:30-17:30) on multiple days in March 2019 and January 2020. The data was collected in January and March to ensure capturing various RW conditions required for the analyses in this study. The observations are made by continuously measuring the headway of queueing vehicles passing through the intersection for each lane. TrafficAnalyzer i.e., a video processing software developed by Suzuki et al. (2016) was used to process the recordings. In this study, the saturated headway is calculated based on the following procedure recommended in the HCM (2016).

1. Manually record the timestamps when the front axle of each vehicle in the queue crosses the stop line at the beginning of the green phase.
2. For each vehicle discharged from the queue, the headway is estimated as the difference between its timestamp and that of its leading vehicle recorded in Step 1.
3. The average headway of the fifth and subsequent queuing vehicles in each cycle is estimated as saturation headways for that cycle as per HCM (2016) definitions. In this study, only queues with eight or more vehicles were considered to ensure the validity of the average headway in each cycle.

In addition to the headway data, three types of vehicle types were also registered based on the *Federal Highway Administration* (FHWA) classification: passenger cars as PCs, single-unit trucks, and articulated trailers (FHWA, 2001). From a sample size standpoint, single-unit trucks and articulated trailers are combined as HVs in this study.

2.3.3 Data Collection for Weather Conditions

RW (road-weather) conditions were classified into 7 categories based on the observations from videographic data and the criteria described below.

- Dry = No moisture, ice and snow are detected on the road surface,
- Partly wet = Moisture is detected in the wheel path,
- Wet = The entire road surface is wet,
- Icy = The road surface is flat, but the road surface is white and frozen,
- Partially snow-covered = The road surface is elevated with dirt snow, and the wheel path is melted,
- Packed snow = More than 80% of the road surface is covered with white snow,
- Snow-covered = The road surface is completely covered with white snow

Field surveys were conducted in only selected days in March 2019 to ensure the consistency of RW classifications. RW condition categories are presented visually in Figure 2.3. To supplement

the classification of RW conditions, essential weather information was also obtained from Environment Canada (Government of Canada, n.d.).

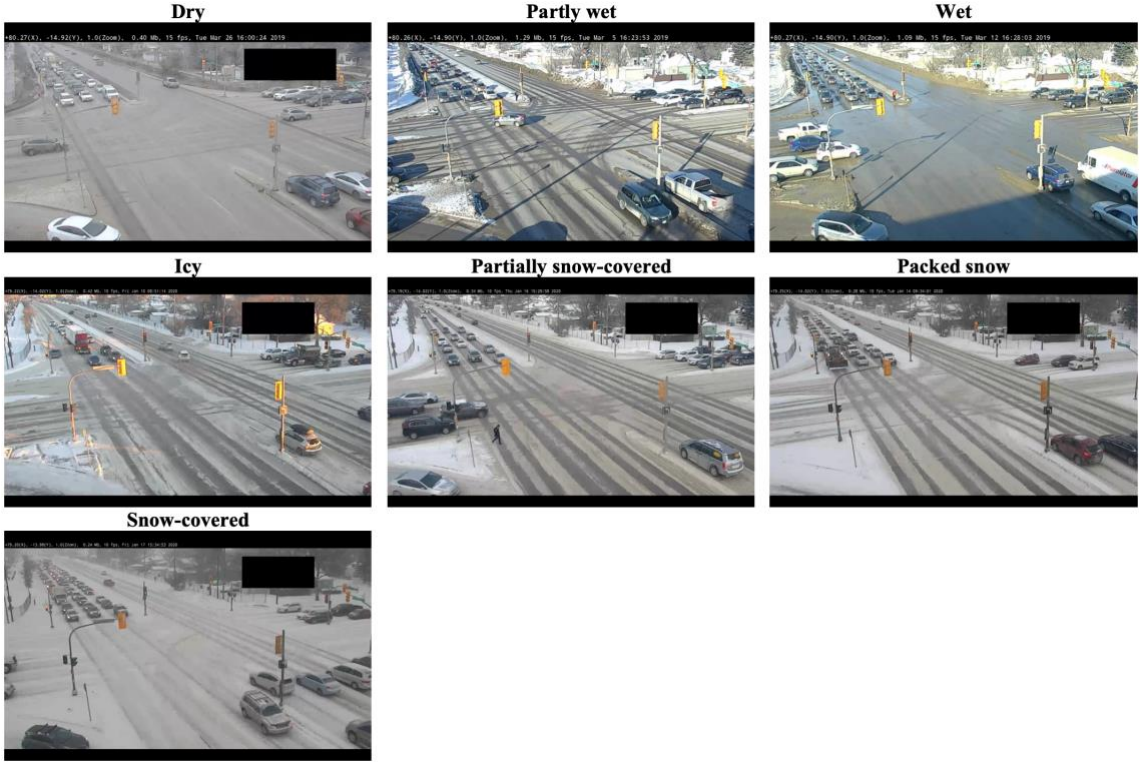

Figure 2.3: Screenshots of RW Classifications at Century

2.4 Preliminary Analysis and Visualizations

2.4.1 Impacts of Road Weather Conditions

Saturation headways measured per cycle were categorized into seven groups as per RW condition classification. In Figure 2.4, the stepped lines show the cumulative percentage of saturation headway frequency at 0.1s increaments. The dotted curves are the modelled probability density functions assuming a normal distribution for saturation headway. Table 2.1 shows the number of cycles, mean values, standard deviations of saturation headways and the increase rate for each intersection and road surface condition. The increase rate can be calculated by dividing the saturation headway difference between Dry and Adverse weather conditions by that of Dry conditions. Generally, observed saturation headways are relatively longer and with higher standard deviations under adverse RW conditions compared to dry conditions. The Dwass Steel all-pairs comparison test for non-parametric data was performed for saturation headways in different groups

(Steel et al., 1960). The results indicated that, for Century, there are significant differences among the mean values of three groups (Dry, Partly wet and Wet), (Icy, Partially snow-covered) and (Packed snow, Snow-covered) at 95% confidence level. For Dugald, significant differences were barely detected between Dry and Partially snow-covered. This observation could be the result of smaller sample size of fewer than 20 cycles. Thus, additional categories were created to combine RW conditions i.e., "Normal" category to combine Dry, Partly wet, and Wet, "Partly snowy" category to combine Icy and Partially snow-covered, and "Snowy" category to combine Packed snow and Snow-covered. At Century, the mean value of the saturation headways for Normal category was 2.02 seconds, while that of Partly snow and Snowy categories were increased by 13.6% and 38.4%, respectively. In the case of Dugald, the mean value of saturation headway increased by 17.6% and 38.7%, respectively, comparing to 1.81 seconds under Normal category. Kolmogorov-Smirnov test (KS test) results in Table 2.2, which uses the maximum absolute difference between the two cumulative distributions (KS stats), confirms that the two groups of Normal and Partly snowy or Snowy were not derived from the same distribution for both intersections.

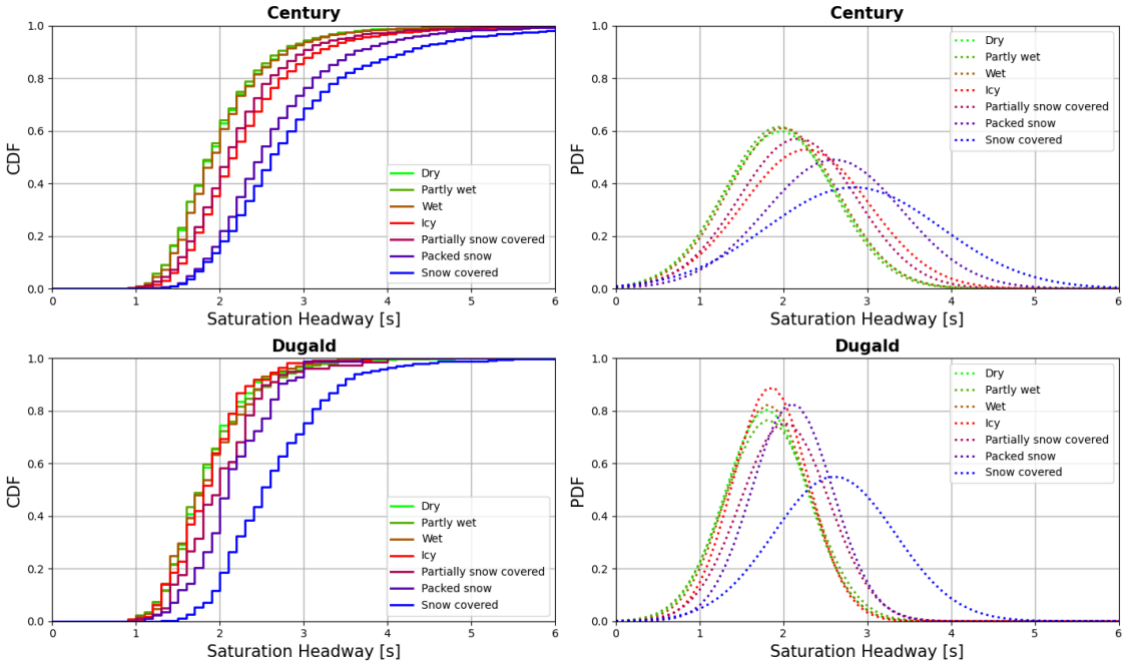

Figure 2.4: Cumulative Density Function (CDF) and Probability Density Function (PDF) of Saturation Headway Distributions at Century and Dugald

Table 2.1: Summary of Collected Data for the Center Lane

RW classifications		Century (Figure 2.1 (a))					Dugald (Figure 2.1 (b))				
		Number of Cycles	Mean headway (s)	Std	Mean headway (s)	Increase rate (%)	Number of Cycles	Mean headway (s)	Std	Mean headway (s)	Increase rate (%)
Normal	Dry	139	2.02	0.72	1.99	-	204	1.93	0.5	1.93	-
	Partly wet	216	1.99	0.71			82	1.97	0.52		
	Wet	155	2.04	0.7			16	2.15	0.49		
Partly snowy	Icy	188	2.34	0.82	2.26	△13.6	16	2.29	0.53	2.27	△17.6
	Partially snow covered	80	2.24	0.9			22	2.27	0.45		
Snowy	Packed snow	74	2.68	0.9	2.75	△38.4	15	2.48	0.49	2.68	△38.7
	Snow covered	108	2.81	1.01			35	2.69	0.73		

NOTE: Std = Standard error

Table 2.2: Kolmogorov-Smirnov Test Results

	Place				Lane types		Vehicle types			
	Century		Dugald		Median vs Center		PC		HV	
	KS stats	P-value	KS stats	P-value	KS stats	P-value	KS stats	P-value	KS stats	P-value
Normal	-		-		0.177	0.000	-		-	
Partly snowy	0.571	0.000	0.330	0.001	0.192	0.000	0.218	0.000	0.110	0.778
Snowy	0.833	0.000	0.823	0.000	0.093	0.514	0.440	0.000	0.201	0.124

NOTE:
[1] The reference of KS results for place and vehicle types are Normal conditions

2.4.2 Degree of Influence of Road Surface Conditions

In this section, the degree of influence of RW conditions on saturation headway is analyzed for each lane and vehicle type. Figure 2.5 represents boxplots of observed saturation headways at Century, where in each box, the height of the box represents interquartile range, the line dividing the box indicates the median, the triangle represents the mean, and the whiskers show the maximum and minimum values (excluding the outliers). Figure 2.5 (a) shows the saturation headway per cycle for the through lanes, which are the median lane next to the median island and the center lane next to the shoulder lane at Century. In Normal and Partly snowy conditions, there was a significant difference between median and center lanes according to the results of the KS test shown in Table 2.2, but no significant difference was observed in Snowy conditions. This may

be caused by the fact that the median lane is usually used as an overtaking lane. Thus, the median lane could potentially represent relatively aggressive driving baviour. However, when snow accumulates on the road, the boundary between the lanes and the median island becomes blurred, and the median lane does not fully function as overtaking lane.

The degree of influence of RW conditions on saturation headway was also investigated considering vehicle types. Figure 2.5 (b) shows the headway distribution for PC-only, i.e., only headways tagged to PC, and HV-only, i.e., only headways tagged to HV, for each RW condition of the center lane at Century, which has sufficient HV samples. Measured headways were labeled as PC-only or HV-only based on the vehicle type observed. It can be seen that saturation headway increased considerably by the vehicle size. In Table 2, headway distributions of each vehicle type are compared using KS test under adverse RW and Normal condition. However, the impact of RW conditions was more pronounced for the PCs, while the observed difference for HVs decreased gradually. Besides, PCE values were calculated using Equation (2.1) from headways and HV ratio under three RW conditions. The PCE values are based on the reduced capacity in each RW category.

$$PCE = \frac{h_s - h_{PC}(1 - P_{HV})}{h_{PC}P_{HV}} \tag{2.1}$$

where

h_s = average saturation headways per cycle

h_{PC} = average headways of only PCs in the cycle

P_{HV} = the proportion of HVs in the cycle

As shown in Table 2.3, the mean PCE for Normal condition was 2.07, that is consistent with default value of 2.0 in HCM (2016) for the HV ratio adjustment. However, mean PCE in Partly snowy and Snowy conditions reduced to 1.72 and 1.47, respectively. The higher standard deviation still exists, but these results support the notion that HVs are less susceptible to adverse RW conditions, when comparing the impact of HVs and PCs on traffic in each RW classification. There is a possibility that the stability of HVs due to their weight and size, as well as higher viewing angle, and the experience of HV drivers result in more stable driving behaviour for HVs at intersections even under adverse RW conditions compared to PCs.

In addition, to see the overall trends between HV ratio and saturation headways for different RW conditions, linear regression models were developed using the least-squares method. The resulting models are shown in Figure 2.6 and the estimated parameters are listed in Table 2.3. Although the coefficient of determination for saturation headway under Snowy conditions is low, the slope of regression lines demonstrate the impact of HV ratio on saturation headway under different RW conditions. Additionally, it can be observed that the impact of HV ratio on saturation headway is less significant as RW conditions aggravated, that is consistent with observations presented earlier. While the regression model coefficients are statistically significant in the headway model, caution is recommended while using these models for field prediction during Partly snowy and Snowy condition since the explanatory values (R-squared) of the models are limited.

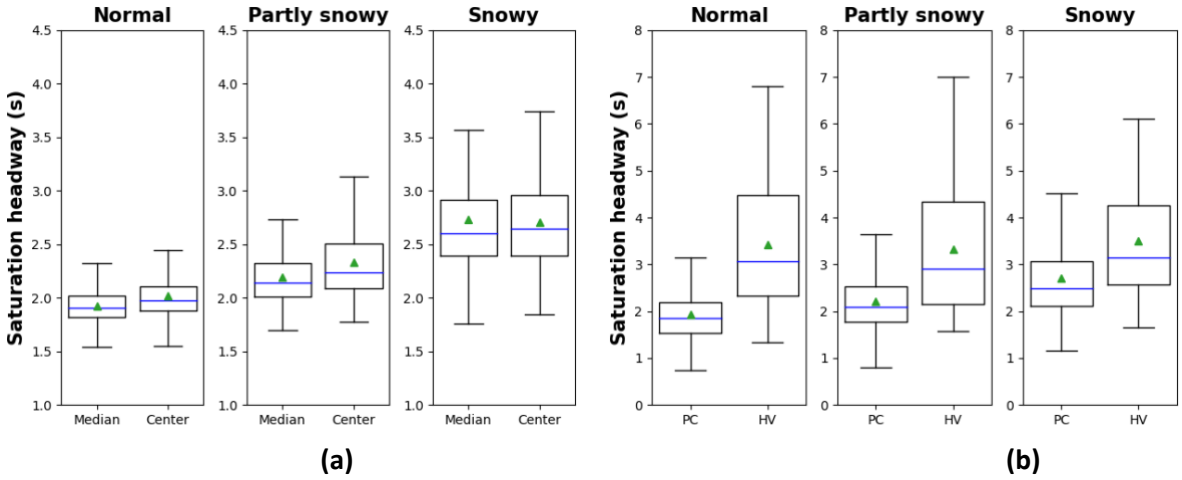

Figure 2.5: Boxplots of Headways at Century: (a) Lane Type and (b) Vehicle Type

Table 2.3: Summary of PCE and Linear Regression Models

	Cycles	PCE		(Saturation headways) = Coef ·(HV ratio) + Intercept			
		Mean	Std	Coef	Intercept	R-squared	P-value
Normal	121	2.07	0.90	0.034	1.93	0.63	0.000
Partly snowy	74	1.72	0.81	0.019	2.23	0.46	0.000
Snowy	51	1.47	0.48	0.011	2.67	0.18	0.005

NOTE: Std = Standard error

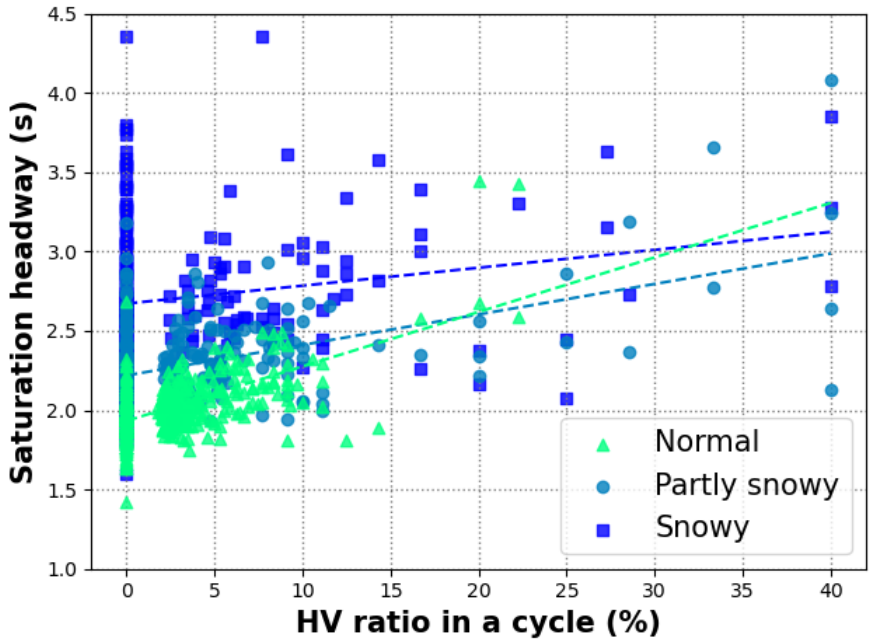

Figure 2.6: Saturation Headway and HV Ratio per Cycle at Century

2.5 Results and Discussions

2.5.1 Saturation Headway Distributions

In the first part of analysis, this paper develops different saturation headway distributions because headway generation is a first step to simulate traffic flow realistically. As shown in Table 2.4, several functional forms can be considered to model saturation headway distribution for through movements. In this study, five alternative models including Normal, Lognormal, Gamma, Logistic, and Weibull distribution functions were examined, and model parameters were calculated using Maximum Likelihood Method. The goodness of fit for each distribution function was evaluated using KS test. In the end, since the P-values of all the models were less than 0.05, the model with the smallest KS statistic was considered the best fitting model. Consequently, the lognormal distribution function defined by Equation (2.2) was found to be the best model for representing saturation headway distribution in all case. Figure 2.7 compares observed cumulative and probability distributions with fitted models using lognormal distribution function for each RW condition under different HV ratios. It can be seen that overall, saturation headway increases as RW conditions degrade and the probability functions become flat, but the difference in the distributions between Non HV-involved headway and HV-involved headway was negligible.

$$f(x) = \frac{1}{\sqrt{2\pi}\sigma x}\exp\left\{-\frac{(\ln x - \mu)^2}{2\sigma^2}\right\} \quad (2.2)$$

$$\mu = \ln\left(\frac{m^2}{\sqrt{v+m^2}}\right), \quad \sigma = \sqrt{\ln\left(\frac{v}{m^2}+1\right)} \quad (2.3)$$

where

m = mean of headway distribution

v = variance of headway distribution

Table 2.4: Evaluation of the Fitting of Headway Distributions

	Distribution Function	Normal			Partly snowy			Snowy		
		KS stats	P-value	Rank[1]	KS stats	P-value	Rank[1]	KS stats	P-value	Rank[1]
NonHV-involved headway	Normal	0.0960	0.0000	5	0.0929	0.0000	4	0.1134	0.0000	4
	Lognormal	0.0344	0.0000	1	0.0412	0.0000	1	0.0591	0.0000	1
	Gamma	0.0501	0.0000	2	0.0541	0.0000	2	0.0747	0.0000	3
	Logistic	0.0605	0.0000	3	0.0569	0.0000	3	0.0736	0.0000	2
	Weibull	0.0865	0.0000	4	0.0978	0.0000	5	0.1162	0.0000	5
	Lognormal parameters	(μ,σ) = (0.4452, 0.3283)			(μ,σ) = (0.9162, 0.2462)			(μ,σ) = (1.0734, 0.2718)		
HV-involved headway	Normal	0.1157	0.0000	5	0.1057	0.0000	4	0.1171	0.0000	4
	Lognormal	0.0382	0.0000	1	0.0472	0.0000	1	0.0620	0.0000	1
	Gamma	0.0619	0.0000	2	0.0634	0.0000	2	0.0780	0.0000	3
	Logistic	0.0689	0.0000	3	0.0639	0.0000	3	0.0764	0.0000	2
	Weibull	0.1081	0.0000	4	0.1153	0.0000	5	0.1174	0.0000	5
	Lognormal parameters	(μ,σ) = (0.4185, 0.3554)			(μ,σ) = (0.8703, 0.2706)			(μ,σ) = (1.0707, 0.2797)		

NOTE:
[1]Rank compares KS stats among the distribution functions with P-value of less than 0.10

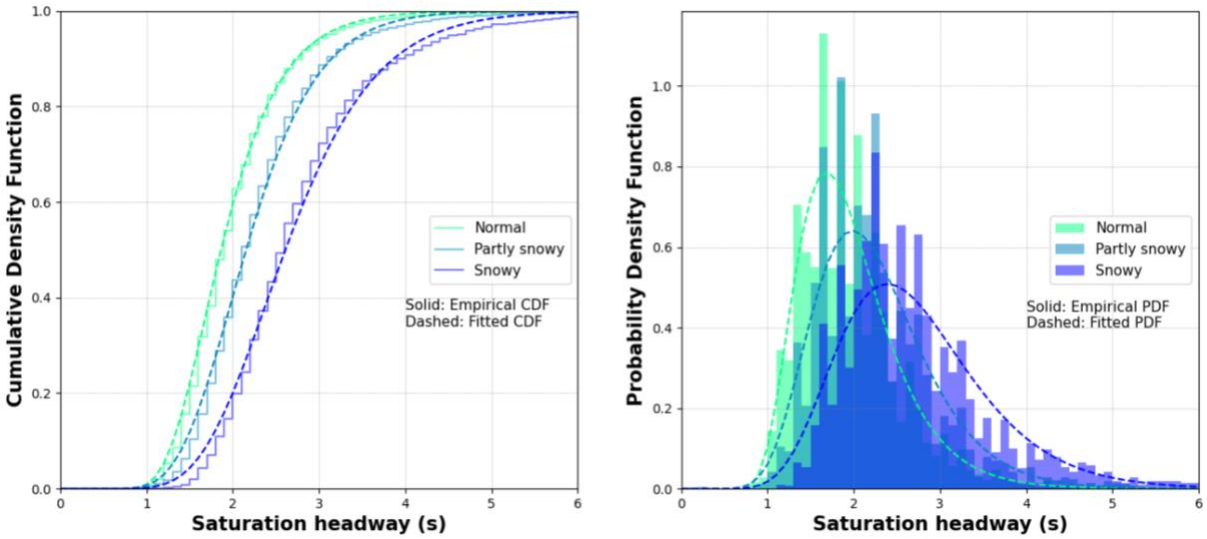

Figure 2.7: Density Functions of the Best Fitted Models (Lognormal Function)

2.5.2 Saturation Headway Models

In this second part of analysis, saturation headways of the through-lane h_s are modelled by multiple regression models using least squared method to assess the simultaneous impact of geometric design and traffic volume on saturation headways. After several iterations considering different explanatory variables including:

- HV ratio (%)
- Partly snowy dummy variable (not Partly snowy=0, Partly snowy=1)
- Snowy dummy variable (not Snowy=0, Snowy=1)
- Time dummy variable (PM=0, AM=1)
- Place dummy variable (Century=0, Dugald=1)
- Lane Width (Difference relative to 12 ft)
- Daytime dummy variable (Daytime=0, not=1)
- Weekend dummy variable (Weekend=0, not=1)
- Temperature (℃),

Independent variables with better prediction power were selected using the stepwise method as shown in Equation (2.4), and a multiple regression analysis was conducted.

$$h_s = \alpha_0 + \alpha_1 x_1 + \alpha_2 x_2 + \alpha_3 x_3 + \alpha_4 x_4 + \alpha_5 x_5 + \alpha_6 x_6 \quad (2.4)$$

where

$\alpha_0 \sim \alpha_6$ = model coefficient

x_1 = HV ratio (%)

x_2 = Partly snowy dummy variable

x_3 = Snowy dummy variable

x_4 = Time dummy variable

x_5 = Place dummy variable

x_6 = Lane Width (ft)

The results of the following three models are shown in Table 2.5:

- Model I for cycles only with PCs
- Model II for cycles with at least one HV
- Model III for all cycles

To compare the degree of influence among the explanatory variables, the t-value ratio (%) was defined for each variable using the following Equation (2.5).

$$(\text{t} - \text{value ratio})_i = 100 \cdot \frac{|t_i|}{\sum_{i=1}^{6} |t_i|} \quad (2.5)$$

where

t_i = t-value for variable i

The P-values and F-values for the majority of explanatory variables were less than 0.000 for all the models, confirming statistical significance of explanatory variables. Considering t-value ratios in each model, Snowy condition was the most influential factor in increasing the saturation headway among all explanatory variables, following by Partly snowy condition (in Model I and Model III), indicating that deteriorating adverse RW condition is a determining factor for saturation headway. It can also be seen that a 1% increase in the HV ratio increases the saturation headway by more than 0.023s (Model III) and 0.029s (Model II). Comparing Model I and Model II, the HV ratio has a 25.9% weight of the total influence. Alternatively, the degree of influence of

Snowy and Partly snowy condition has decreased. This alludes to the fact that the influence of the mixture of HVs and the influence of RW condition is comparable.

In addition to these observations, when the Daytime dummy (defined as the time from sunrise to sunset) was used as an explanatory variable, the P-value was 0.229, i.e., rejecting its significance. On the other hand, the Time dummy had a significant effect, suggesting that driving behaviour at AM was more aggressive than PM, and drivers tended to hurry during morning peak regardless of the brightness of the daylight. The negative sign of model coefficient for lane width reveals that expanding the lane width can decrease saturation headways. However, it should be noted that only the range from 12ft to 13ft is applicable.

Overall, the adjusted coefficient of determination in Model III i.e., 0.544 , indicates the significant relationship between independent and dependent variables. The Mean Absolute Percentage of Error (MAPE) calculated by Equation (2.6) is 8.49% in the Model III. Figure 2.8 illustrates the comparison between the observed and estimated saturation headway values. Besides, according to the Root Mean Squared Percentage of Error (RMSPE) of 11.9% provided by Equation (2.7), this proposed regression model could be further improved. Especially, the proposed model tends to underestimate the saturation headways, as the saturation headway per cycle becomes large, and the deviation also becomes more significant under adverse weather conditions. These errors may be due to inter-relationships between various factors triggered by individual variations in driving behaviour under adverse RW conditions.

$$\text{MAPE} = \left(\frac{100}{N} \sum_{i=1}^{N} \frac{|x_i - \widehat{x_i}|}{x_i} \right) \tag{2.6}$$

where

x_i = Observed saturation headways (s)

$\widehat{x_i}$ = Estimated saturation headways (s)

$$\text{RMSPE} = \left(\sqrt{\frac{100}{N} \sum_{i=1}^{N} (x_i - \widehat{x_i})^2} \right) \tag{2.7}$$

where

x_i = Observed saturation headways (s)

$\widehat{x_i}$ = Estimated saturation headways (s)

Table 2.5: Results of Multiple Linear Regression

Variables	Range or Frequency	Sig[2]	Estimated Parameters		Std	t-value	t-value ratio (%)
Model I (Except HV containing cycles)							
Intercept	na	na	α_0	1.952	na	na	na
Partly snowy dummy	450 cycles	*	α_2	0.327	0.016	20.631	22.6
Snowy dummy	291 cycles	*	α_3	0.857	0.019	44.473	48.7
Time dummy (PM=0, AM=1)	173 cycles	*	α_4	-0.350	0.024	-14.637	16.0
Place dummy (Century=0, Dugald=1)	368 cycles	*	α_5	-0.156	0.018	-8.864	9.7
Lane width (ft) [3]	0 ft -1 ft	*	α_6	-0.039	0.014	-2.809	3.1
Number of observations (cycles): 1898 Prob(F-stats): 0.000	Adjusted R-squared: 0.548 MAPE: 8.24% RMSPE 10.87 %						
Model II (HV containing cycles)							
Intercept	na	na	α_0	1.998	na	na	na
HV ratio (%)[1]	0% < - ≤ 50%	*	α_1	0.029	0.003	9.194	25.8
Partly snowy dummy	89 cycles	*	α_2	0.283	0.054	5.877	16.5
Snowy dummy	62 cycles	*	α_3	0.560	0.048	9.504	26.7
Time dummy (PM=0, AM=1)	57 cycles	*	α_4	-0.453	0.059	-5.911	16.6
Place dummy (Century=0, Dugald=1)	22 cycles	*	α_5	-0.252	0.077	-3.261	9.1
Lane width (ft) [3]	0 ft -1 ft		α_6	-0.103	0.054	-1.900	5.3
Number of observations (cycles): 314 Prob(F-stats): 0.000	Adjusted R-squared: 0.418 MAPE: 9.72% RMSPE 12.56 %						
Model III (All cycles)							
Intercept	na	na	α_0	1.966	na	na	na
HV ratio (%)[1]	0% ≤ - ≤ 50%	*	α_1	0.023	0.001	19.443	17.3
Partly snowy dummy	539 cycles	*	α_2	0.326	0.015	21.210	18.8
Snowy dummy	353 cycles	*	α_3	0.812	0.019	43.298	38.4
Time dummy (PM=0, AM=1)	230 cycles	*	α_4	-0.362	0.023	-15.874	14.1
Place dummy (Century=0, Dugald=1)	390 cycles	*	α_5	-0.164	0.018	-9.320	8.3
Lane width (ft) [3]	0 ft -1 ft	*	α_6	-0.048	0.014	-3.501	3.1
Number of observations (cycles): 2212 Prob(F-stats): 0.000	Adjusted R-squared: 0.554 MAPE: 8.49% RMSPE 11.19 %						

NOTE: Std = Standard error, na = not applicable

[1] The maximum HV ratio is 50%

[2] (*) indicates significant variables with 95% of significance level (P-values < 0.05)

[3] Lane width indicates the difference from 12 ft

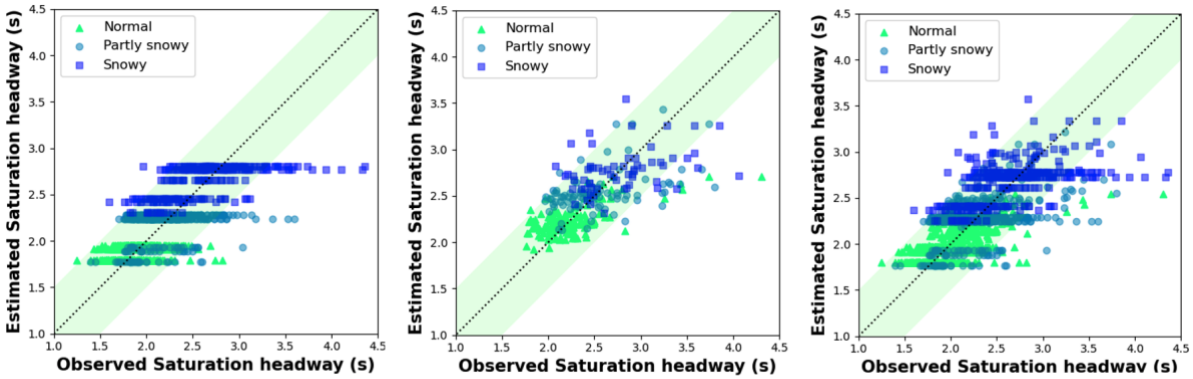

Figure 2.8: Comparison between Observations and Estimations

2.6 Conclusions

In this paper, variations of saturation headway at signalized intersections was investigated under different adverse RW(road-weather) conditions and HV (heavy vehicle) ratios. In addition, regression models were developed to describe saturation headway as function of adverse RW conditions and HV ratios. Road surface condition was the dominant factor causing from 13.6% to 38% longer headways in Partly snow and Snowy conditions. Under Normal conditions (i.e., either dry, partly wet, and wet), the average saturation headway on the lane adjacent to the median island was 5% shorter than that of the center lane. However, the difference in saturation headway across the lanes became less significant in adverse RW conditions, which could be attributed to blurred boundary between the lanes as a result of snow accumulation and reduced overtaking through median lane. Saturation headway distributions found to follow left-skewed lognormal functions with different parameters demonstrating increased variance as RW conditions worsened.

In addition, a comparison of the headway among vehicle types showed that HVs required an average of 84% longer headway than PCs (passenger cars). Conversely, the measured relative PCE (passenger car equivalent) i.e., the number of PCs equivalent to one HV in view of headway in each RW category, under Normal was 2.07, while it was 1.72 for Partly snowy and 1.47 for Snowy, which indicates that HVs are less sensitive to road conditions than PCs. The multiple regression model estimated in this study, with statistically significant variables and a MAPE (mean absolute

percentage of error) of less than 10%, is able to estimate the saturation headway according to the HV ratio under different RW conditions. The presence of HVs in cycles itself is found to significantly increase the saturation headway of each cycle; consequently, the agglomerated effects with RW conditions clearly imply that they have notable implications of reducing the performance of signalized intersections. The findings of this study are expected to be helpful for the review of traffic volume and the estimation of saturation flow rate in signalized intersections where heavy vehicles often travel in severe snowfall conditions.

In closing, as with any research effort, this study has its limitations and the findings open the window for many research extensions that warrants attention. For instance, this paper has used data from two signalized intersections in Winnipeg, Manitoba and large-scale data collection efforts covering multiple regions will be required to test the geographical stability of saturation headway distributions and models. On the other hand, there is also a possibility of human-oriented errors in the data collection since pavement conditions and headway data are extracted from the video recordings manually. The future scope of this study is to explore non-linear model specifications to more accurately represent and predict saturation headways. Furthermore, it is also imperative to explore how the saturation headways can be converted to traffic capacity based on the results of this study and to examine the extent to which the study findings are transferable to other geographic locations. The long-term outcomes of this research will help to produce a more generalized signal plan that adapts to the different road weather conditions and HV ratio, and in turn to improve the traffic capacity and delay conditions at signalized intersections.

3 IMPLEMENTING SURVIVAL ANALYSIS TO CAPTURE STOCHASTIC CHARACTERISICS OF SATURATION FLOW RATE

This chapter begins with the proposal of a stochastic concept of SFR, which take the unsaturated vehicles into account of SFR distributions. It aims to cast doubt on the general approach to measuring SFR and provide alternative solutions. Then, statistical methods will be demonstrated to define a threshold of saturation in a waiting queue. The analysis of this chapter contributes to the production of realistic SFR distributions. The reliable and malleable methodology of SFR estimations will give traffic engineers options to adjust the signal setting and improve WRTM.

The material in this chapter is original for this thesis. The thesis author conducted the analysis, interpreted results, and prepared the manuscript. The chapter consists of own abstract, introduction and conclusion; acknowledgements and references are provided at the end of the thesis. A duplicated section with Chapter 2 on data collection were removed from the original paper to allow smooth integration.

3.1 Abstract

Saturation flow rate (SFR) is a key parameter in estimating the capacity of signalized intersections and is known to be affected significantly by adverse road-weather (RW). To measure SFR from observed headways and demonstrate the effect of RW conditions, existing studies often focus on estimating a deterministic value for SFR by considering the mean saturation headway observed on and after a critical vehicle (CV), interpreted as the threshold to observe the saturated flow empirically, i.e., 5th vehicle in the queue. However, the conventional approach fails to consider the stochasticity associated with SFR due to variability in driver behaviour and neglects the additional (i.e., censored) information on SFR provided by vehicles observed in the unsaturated portion of the queue. Moreover, the common practice to consider a pre-defined CV to estimate SFR is limiting as it does not consider the variations in vehicle type, driving behaviour, and other prevailing conditions. Flow rates in about 1,000 cycles were extracted from video recordings of a signalized intersection in Winnipeg, Canada, to investigate the implications of adverse RW conditions on SFR distributions and CV. By implementing survival analysis method, stochastic

SFR distribution functions, which adequately deal with the censored data, are modelled. Besides, a statistical approach for reasonably determining an optimal CV is proposed. The analysis findings suggest that adverse RW conditions decrease SFR significantly, moves CV to the front of the queue and do not show a significant effect on SFR for heavy vehicles (HV) compared to passenger cars (PC). Furthermore, this study implies that the conventional deterministic approach overestimates the probability of saturation at a given flow rate. The proposed analysis method reveals stochastic characteristics of SFR and provides a methodological approach to model SFR distributions under different RW conditions, which is essential for improving the operation of signalized intersections, particularly in cold regions.

Keywords: Saturation flow rate; Saturation headway; Survival analysis; Adverse road-weather; Heavy vehicles

3.2 Introduction

Intersection capacity analysis is crucial for engineering decisions about the design, planning, and operation of supply-demand imbalance in roadways. SFR (Saturation Flow Rate) determination is a major part of intersection capacity analysis which quantifies the rate at which vehicles cross the stop line of a signalized intersection approach lane during the green interval (ITE, 2007). In the signal timing design and operation guidelines, when planning and designing signalized intersections, SFR for a specific lane (or lane group) is considered one constant value and estimated considering a base SFR (veh/h), i.e., 1,900 (veh/hour/lane) for through lane as per HCM (Highway Capacity Manual) 6th edition (TRB, 2016). To capture the SFR at a specific location, the base SFR is adjusted by intersection geometry (e.g., lane width and grade), traffic flow characteristics (e.g., right/left turn volume and traffic composition), and lane utilization pattern (TRB, 2016). Besides, SFR is the inverse of saturation headway (SH) which can be measured empirically. To convert empirically observed SH to SFR, the several HCM editions i.e., 3rd to 6th (TRB, 1985, 2000, 2010, 2016) suggest estimating the mean SH at the onset of green phase using the headways associated with the 5th vehicle (critical vehicle) in the queue onward until the standing queue dissipates, as shown in Figure 3.1 (TRB, 2016). Discarding the discharge headways of the first four vehicles is based on the past empirical results, which indicates that start-up lost time is present for the first

few vehicles in the queue but disappeared after the 4th vehicle. Hereafter this concept is called HCM method.

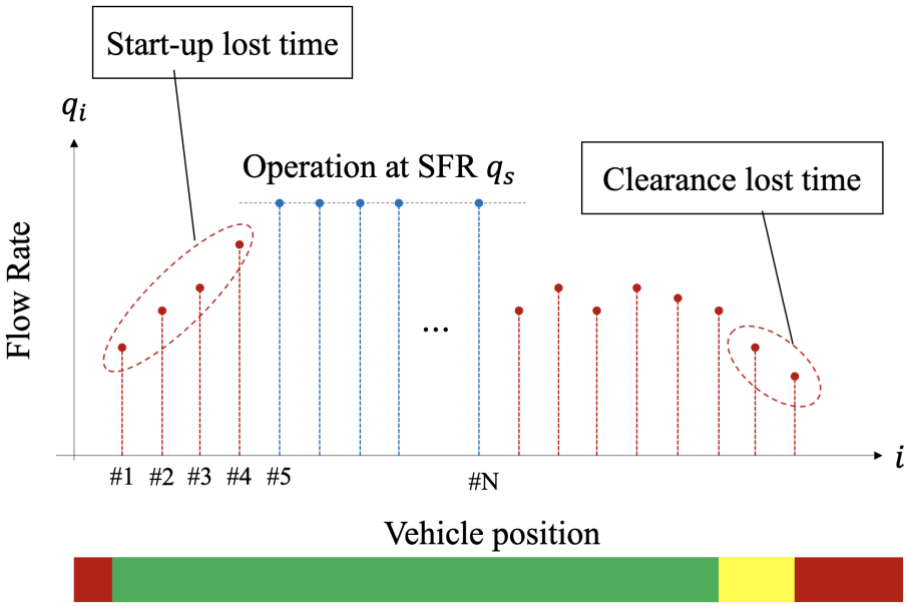

Figure 3.1: Conceptual Illustration of SFR

However, there are several underlying research gaps that need to be contemplated regarding the concept of SFR and its conventional calculation approach;

1. *SFR is considered deterministic.*

   When SFR is calculated or estimated, the outcome comes down to one specific value representing the maximum flow per cycle. However, we anticipate that the maximum flow per cycle may possess stochastic characteristics due to the impacts of RW (road-weather) conditions, vehicle composition, i.e., HV (heavy vehicle) percentage, and driver behaviour (Hirose et.al., 2022).

2. *Neglecting the potential information on SFR provided by the first fourth vehicles in the queue.*

   HCM method discards the first four vehicles (unsaturated vehicles) from SFR calculation to account for the start-up lost time. Yet, unsaturated flow can potentially provide useful information about the saturated flow. For instance, SFR is always greater than unsaturated flow rate. Statistical methods for survival data analysis can be used to effectively

incorporate the information provided by such "censored" data of unsaturated vehicles into SFR estimation.

3. *The reasoning for considering the "5th vehicle" as a critical vehicle (CV) is not well-justified.*

   In most existing research, which attempts to measure SFR at signalized intersections, the threshold for observing the SH is based on considering the 5th vehicle in a queue as CV. Furthermore, the concept of CV as HCM 6th recommends is based on empirical observations under ideal RW conditions (TRB, 2016). Thus, the methodology to find the optimal CV is not well-established.

Given the above-noted gaps and shortcomings, this study aims to provide a probabilistic approach to estimating SFR by considering the effect of "unsaturated vehicles" at the beginning of the queue. In doing so, implementation of survival analysis approach is attempted. In addition, the derived distributions for SFR are compared with respect to adverse RW conditions, vehicle types and CV positions. Finally, optimal CVs are identified under different RW conditions and the procedures to find the location of CV in the queue are suggested. The findings in this paper are expected to establish a new concept of the stochastic SFR and challenge the conventional SFR calculation approach, especially where comparable cold RW and HV (heavy vehicles) ratios play a significant role in traffic performance.

The remainder of the paper is structured as follows: the next section introduces the past studies related to the SFR calculations, the variance due to RW conditions and HV's implications and the use of survival analysis in traffic studies. The following section summarizes how to extract SFR and RW conditions from the sourced data. Then after describing how to implement the survival analysis approach to SFR analysis in the subsequent section, derived stochastic SFR distributions are compared, and the methodologies to determine the optimal CV are proposed in the penultimate paragraph. The last section concludes the paper.

3.3 Literature Review

3.3.1 Variation in SFR

Several studies have been conducted for the field measurement of SFR at specific signalized intersections with the aim of analyzing the saturated state of traffic flow considering different RW conditions, traffic composition, and the position of the critical vehicle in the queue. The majority of the initial studies focused on predicting SFR, proposing values ranging from 1,500 to 2,500 passenger car per hour green time per lane: pcphgpl (Chaudhry, 2013). In one of the first studies conducted in Fairbanks, Alaska, subfreezing conditions in Fairbanks, Alaska (i.e., with ice, snow or frost condition), Botha et al. (1992) expanded on the HCM 3rd (TRB, 1985) for broader applicability. They discovered that the winter SFR was 27% lower than the ideal RW conditions. Besides, they found that the difference in calculating SFR starting at critical vehicle three versus five is insignificant, although no statistical grounds were provided. Lu et al. (2019) quantified RW impacts on signal design-related traffic parameters, including SFR, start-up lost time and free-flow speed, by analyzing traffic video footages of a signalized intersection, in Waterloo, Canada. To extract the headway information associated with SFR, the authors adopted the HCM 5th (TRB, 2000) field measurement technique and found that the SFR decreased from 1,825 (veh/h/lane) to 1,363 (veh/h/lane) due to the snowy RW conditions as compared to normal RW, while start-up delay mainly remained unchanged. Chodur et al. (2011) calculated SFR based on HCM 5th method on Polish intersections and investigated the effect of dry, rainy, cloudy and snowy conditions. Their research explained that adverse RW conditions, even cloudy environments, yielded a shorter initial interval during which start-up lost time appeared and a shorter middle interval, i.e., the interval during which SH becomes stabilized in a cycle. Hirose et al. (2022) previously explored the combined effect of adverse RW and HV presence on saturation headways at signalized intersections. Their research showed that snowy RW conditions increase saturation headway by up to 38.7 % compared to normal conditions. Furthermore, the calculated passenger car equivalent factors and regression models for HV ratio implied that HVs are less sensitive to weather events than PCs (passenger cars). Luo et al. (2019) collected headways from five busy signalized intersections in Guanzhou, China. They analyzed the headway distributions in the different positions in a queue to see the stability of the distributions. They confirmed that average headway gradually decreased with the positions to the 5th vehicle but became stabilized until the 8th vehicle.

3.3.2 Concept and Methodology of Survival Analysis

Survival analysis is commonly used, as the name conveys, to investigate lifetime distributions. The survival function $S(t)$ simply indicates the probability that the end of an event has not yet happened by the time t. As Equation (3.1) shows, the function is the probability that the time to death denoted by T is longer than the time of observation. Thus, the distribution function of a lifetime can be shown in Equation (3.2):

$$S(t) = \Pr(T > t) \tag{3.1}$$

$$F(t) = \Pr(T \leq t) = 1 - S(t) \tag{3.2}$$

where

$S(t)$ = survival function with respect to time t

T = lifetime

$F(t)$ = distribution function of Lifetime

Using the survival analysis to produce lifetime distributions also allows considering the data, which is often censored for reasons such as dropping out of the samples. Treating censored data as missing values would result in biases in the resulting lifetime distributions. On the other hand, by considering the subjects who are still alive at the end of the investigation, a more accurate lifetime distribution can be obtained. To deal with censored data, Kaplan and Meier (1958) have suggested a non-parametric method to produce survival functions that is known as Product-Limit Method (PLM) as in Equation (3.3). In the PLM, censored data are included in the number of total cases until the event occurs and are excluded from the total case after the event.

$$F(t) = 1 - S(t) = 1 - \prod_{i:t_i < t} \frac{n_i - d_i}{n_i} \tag{3.3}$$

where

n_i = the number of individuals with a lifetime $T \geq t_i$

d_i = the number of deaths at a time t_i

Survival analysis has been used frequently in health science studies to investigate the lifetime of participants after medical events, e.g., cancer detection. For example, LaVela et al. (2007)

investigated the lifetime of veterans with spinal cord injuries and disorders. Their multivariable regression models firstly found that the individuals with impairment in the spinal cord tend to have frequent hospital admissions and a higher risk of nosocomial infections. Then, the subsequent survival analysis by the PLM approach was used to explore their lifetime after the infection for three years. The cohort study found that individuals without nosocomial infections lived 11.7 % longer than those who underwent the infections on average. The lifetime distributions for patients with and without infection could inform of not only "dead" or "alive" but also how the survival rate shifts over the experiment, considering patients whose footprints could not be followed.

Beyond typical applications in health science studies, survival analysis is widely applied to other research areas. Yet, its application to traffic studies is relatively new. Schoenfelder and Axhausen (2000) applied survival analysis to model travel rhythms by calculating the probability of occurrence for 23 types of trips (e.g., shopping and active sports) within two weeks based on a six-week continuous travel diary. They discussed that limited duration of investigation often produces incomplete observations, but they could reasonably model the periodicity of everyday life by implementing the survival analysis method. Brilon et al. (2005) proposed a new insight into the understanding of highway capacity. They studied some basic sections of German freeways and produced distribution functions for highway capacity by taking advantage of the survival analysis, precisely PLM. They highlighted the difficulties in directly measuring highway capacity due to the fact that the transition state between the fluent and congested flow is less likely to be observed along the freeway sections. The research implemented the survival analysis to see the capacity distribution for roadways by observing traffic volumes and space mean speeds. They indicate that the stochastic approach permits to utilize of the data observed at lower traffic volume in uncongested traffic, which also delivers essential information regarding highway capacity (highway capacity is greater than observed volumes in uncongested traffic). Their study has confirmed that the observed capacity in the field is lower than the theoretical capacity that assumes ideal conditions. Further, their observations showed that wet road surface reduces the capacity by about 11% in specific study locations. With the application of PLM developed by Brilon et al. (2005), Chauhan et al. (2019) extended the study to investigate the effect of side frictions, like on-street parking and pedestrian movement, on the degradation of the capacity along Indian road sections. Their research suggested that the existence of on-street parking caused a reduction in the

carriageway capacity by up to 12%. The authors further advocated that the implementation of PLM was a powerful tool to allow considerations for stochastic nature of highway capacity instead of providing a discrete and deterministic value, as per the purpose of the analysis.

A review of existing studies endorses the importance of further studying SFR under adverse RW conditions considering the impact of HVs at signalized intersections. Yet, the majority of existing research relies on the HCM method and its definition for saturated traffic that assumes SFR can be observed only after a certain CV, i.e., 5^{th} in the HCM method. A few studies have questioned the traditional HCM method to measure SFR and its applicability under adverse RW conditions. We anticipate that SFR possesses stochastic characteristics similar to highway capacity that is due to variations in driver behaviour, traffic compositions, and environmental conditions. To fill these gaps, we propose to apply the survival analysis to explore stochastic characteristics of SFR, which allows the development of SFR distribution curves under different RW conditions, HV percentage, and considering different positions in the queue for the CV.

3.4 Methodology

3.4.1 Proposed Methodological Advancement to SFR Analysis

In an analogy to the lifetime analysis, the calculation of SFR as indicated by the HCM method ignores the censored data of the first four vehicles in the queue as they are always eliminated from the SFR calculation, resulting in bias in estimation of SFR. We anticipate that by using the survival function in Equation (3.4) a more realistic SFR distributions can be derived by considering the unsaturated vehicles. The analogy between lifetime analysis and SFR analysis is summarized in Table 3.1. In the lifetime analysis, a variable is time, and the breakdown is defined when observing deaths at time t. Meanwhile, SFR analysis uses flow rate q as a variable, and the failure event is observing saturated state at a specific flow rate.

$$S(q) = \Pr(q_s > q) = 1 - F(q) \tag{3.4}$$

where

$S(q)$ = survival function with respect to flow rate q

q_s = SFR

$F(q)$ = distribution function of SFR

Table 3.1: Lifetime Analysis vs SFR Analysis

	Lifetime analysis	SFR analysis
Parameter	Time t	Flow rate q
Failure event	Deaths at time t	Saturated state at flow rate q
Lifetime variable	Lifetime T	SFR indicated as q_s
Censoring	Lifetime T is longer than the duration of the experiment	q_s is greater than the observed flow rate q
Survival function	$S(t) = \Pr(T > t)$	$S(q) = \Pr(q_s > q)$
Probability distribution function	$F(t) = 1 - S(t)$	$F(q) = 1 - S(q)$

3.4.2 Determination of SFR Survival Functions

The survival functions of SFRs were determined in this study by the three-step computational approach explained below.

Step 1: Define the fundamental setting

In this initial step, the data extracted from video recordings and RW information were labelled accordingly: RW conditions (Normal, Partly snowy or Snowy), CV (from 2 to 10) and vehicle type specifications, namely Passenger Car (PC) or Heavy Vehicle (HV). To ensure minimum sample size across categories, this paper excluded the potential effect of clearance lost time by defining the 15th vehicle as the longest queue, which could be cleared within the green phase under any RW conditions. Further, this analysis mostly focused on the flow rates of PCs first and later extended the scope into other vehicle types. The notations considered for this step are listed below.

Notation	Description
i	Vehicle ID in a queue at the beginning of the green phase ($1 \leq i \leq 15$)
j	Cycle ID
c	CV ($2 \leq c \leq 10$) i.e., the position of CV in the queue

Step 2: Production of a survival function for each cycle *j*

To extract a survival function per cycle, which is a set of survival rates, a queue in each signal cycle was classified into 2 states as described in Figure 3.2. State A, which refers to the vehicles

after the CV ($i \geq c$), was considered saturated. State B, which refers to the vehicles before the CV ($i < c$), was regarded as undersaturated.

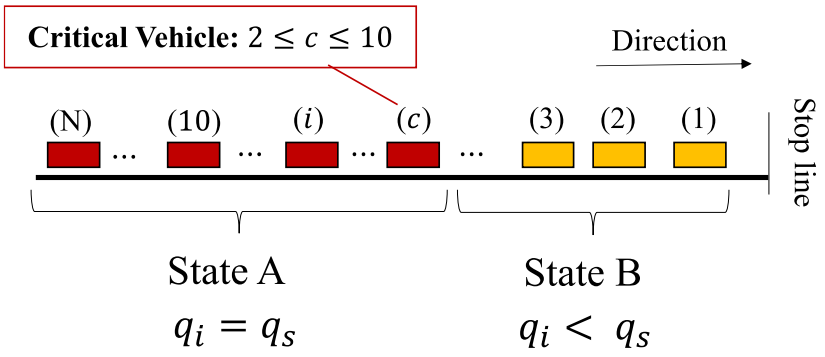

Figure 3.2: Schematic Representation of Flow Rates in a Queue

After the labelling of the saturation state, the entire dataset (A∪B) was sorted by flow rates (i.e., inverse of observed time headway) in ascending order, and as shown in Equation (3.5) the numbers of n_i and d_i were counted to calculate $Prob_j[i]$, which is the probability that vehicle i is unsaturated at the observed flow rate.

$$Prob_j[i] = 1 - \frac{d_i}{n_i} \tag{3.5}$$

where

$Prob_j[i]$ = probability that the vehicle i in cycle j is unsaturated at the observed flow rate

n_i = the number of vehicles labelled with a flow rate $q_s \geq q_i$

d_i = the number of saturated vehicles at a flow rate of q_i

Following to this, the survival rate of vehicle i in cycle j, denoted by $S_j[i]$, is produced by Equation (3.6). The initial survival rate i.e., $S_j[0]$ is always equal to 1.0.

$$S_j[i] = Prob_j[i] \cdot S_j[i-1] \tag{3.6}$$

where

$S_j[i]$ = survival rate ($1 \leq i \leq N_j$) (i.e., probability that the vehicle i in cycle j is unsaturated until the observed flow rate)

N_j = last vehicle ID in a queue for cycle j (max N = 15)

Survival function $S_j(q)$, i.e., $\left[S_j[1], S_j[2], \cdots, S_j[N]\right]$, and the corresponding distribution function of SFR, i.e., $F_j(q)$ are consequently derived as in Equation (3.7)

$$F_j(q) = Pr_j(q_s \leq q) = 1 - S_j(q) = 1 - \prod_{i:q_i < q} \frac{n_j[i] - d_j[i]}{n_j[i]} \tag{3.7}$$

where

$S_j(q)$ = survival function with respect to flow rate q for cycle j

$F_j(q)$ = distribution function of SFR for cycle j

Step 3: Change the settings and repeat the computation

In this step, various SFR distribution functions are derived considering RW conditions, different CV position in the queue, and the vehicle type.

3.5 Results and Discussions

3.5.1 Saturation Flow Rate (SFR) Analysis

From the collected headway data, the means of observed flow rates corresponding to vehicle positions in the queue (from 2nd to 18th having over 30 cycles) were calculated for the three RW conditions. Flow rates were estimated using Equation (3.8), and the mean values are shown in Figure 3.3.

$$q_i = \frac{3600}{h_i} \tag{3.8}$$

where

q_i = flow rate corresponding to observed headway of vehicle i

h_i = headway between vehicle i and vehicle $i - 1$

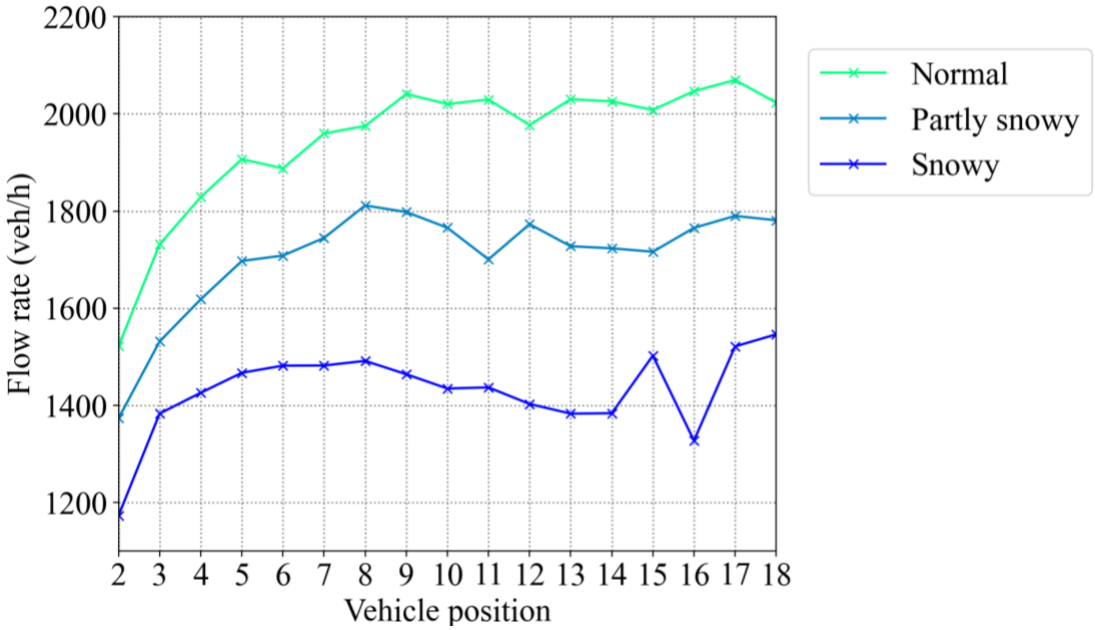

Figure 3.3: Average Flow Rate at Each Vehicle Position in a Queue

Preliminary results show that snowy RW reduces the flow rates significantly. As a case in point, a CV of 5th vehicle indicates the following SFR values under Normal, Partly snowy and Snowy respectively: 1,931 (veh/h/lane), 1,691 (veh/h/lane) and 1,430 (veh/h/lane). The results were also in line with the assertions in HCM since the first several vehicles were associated with substantial reductions in flow rates due to the start-up lost time, and then observed flow rates tend to stabilize with some fluctuations.

The conventional HCM method to calculate SFR was investigated assuming different CVs. As can be seen in Figure 3.4, the stepped curves represent the cumulative distribution functions (CDF), i.e., cumulative percentage of SFR frequency at 1.0 (veh/h) increments, which were calculated deterministically by changing the CV's setting from 2nd to 10th. The SFR under the Snowy RW appears to be markedly lower than Normal RW condition. SFR appears to increase as the CV moves towards the back of the queue under any RW conditions indicating that SH gradually decreases with CV position in the queue. On the other hand, the curves which as based on different CVs overlap closely in Snowy RW conditions. This observation shows that the implication of the reduced flow rate associated with the first part of the queue (unsaturated vehicles) under Snowy

conditions is less significant than that of Normal conditions because Snowy RW results in longer headways even in the beginning of the queue.

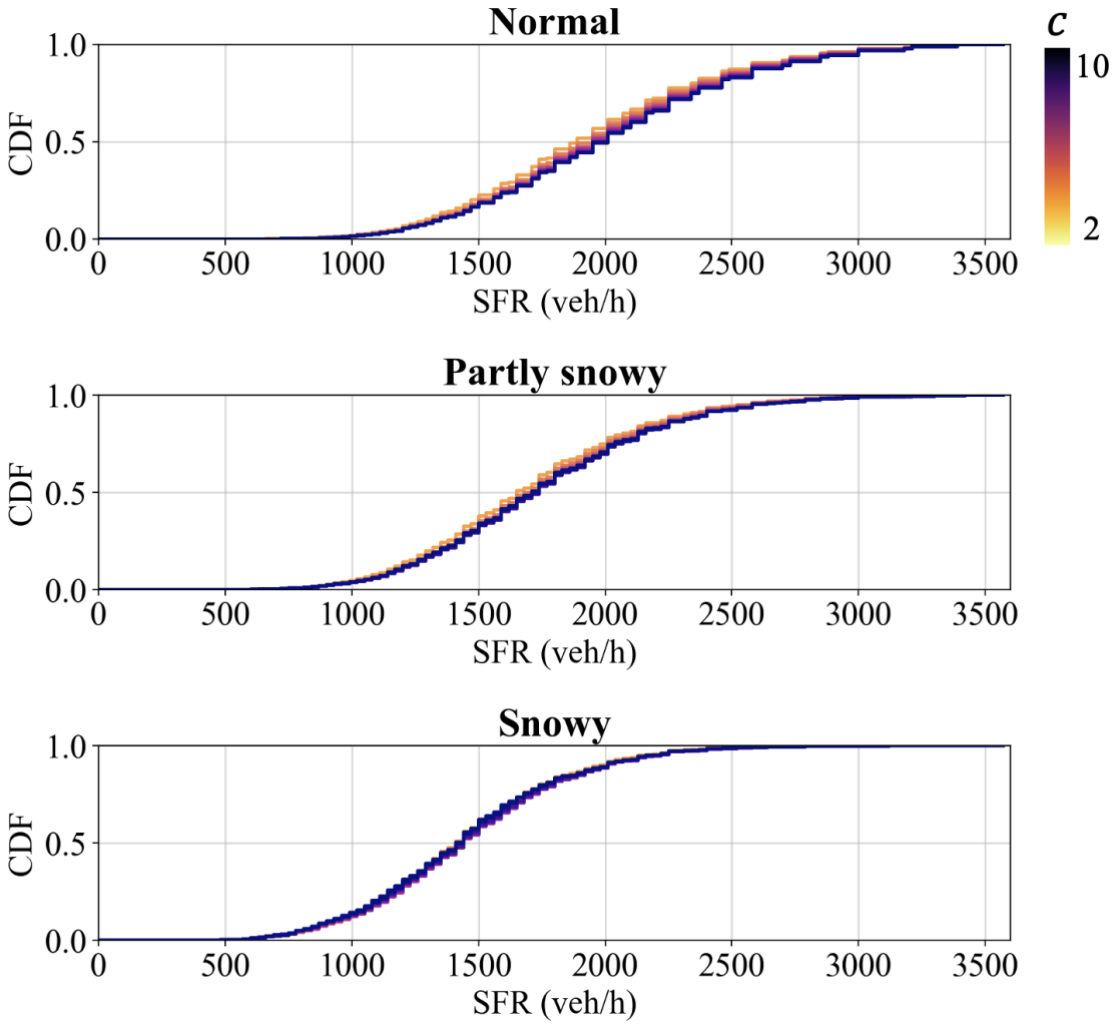

Figure 3.4: Deterministic CDF (Cumulative Distribution Function)

The stochastic distribution functions of SFR were also estimated in this section to quantify the extent of improvement in SFR calculation over the conventional deterministic approach. Figure 3.5 shows per cycle survival functions, which indicate the probability that an observed flow rate is unsaturated, under different CV settings and RW conditions. As can be seen, Snowy RW appears to significantly decrease the unsaturation rate probability (Y-axis); in other words, Snowy conditions define the saturated state at lower flow rates than Normal conditions. Figure 3.6

compares the Weibull fitted distribution functions of SFR for CVs. To have a single line under each assumption, the targeting cycles are combined. The Weibull model is shown in Equation (3.9), and fitting parameters were estimated in the maximum likelihood estimation method and presented in Table 3.2.

$$\hat{F}(q) = 1 - \exp[-\left(\frac{q}{\lambda}\right)^{\rho}] \tag{3.9}$$

where

$\hat{F}(q)$ = Weibull estimated distribution functions with respect to flow rates q

λ = scale parameter

ρ = shape parameter

A horizontal comparison in Figure 3.6 and scale parameters λ clearly shows that the distribution shifts significantly to the right as the CV number increases indicating that flow rates have an increasing trend with CV positions as the interpretation of deterministic curves in Figure 3.4. Comparing the longitudinal difference due to CV among RW conditions, it is observed that the difference is larger with snow for one specific observed flow rate. For example, when 2,000 (veh/h) is observed under Normal conditions, the traffic is saturated with 55 % or 25 % of likelihood with the assumption of 2nd or 10th as a CV. In contrast, they are 87 % or 52 % under Snowy RW. This result alludes to the fact that Snowy conditions bring a higher variance of the probability, and the impacts of unsaturated vehicles to be considered increased on Snowy RW.

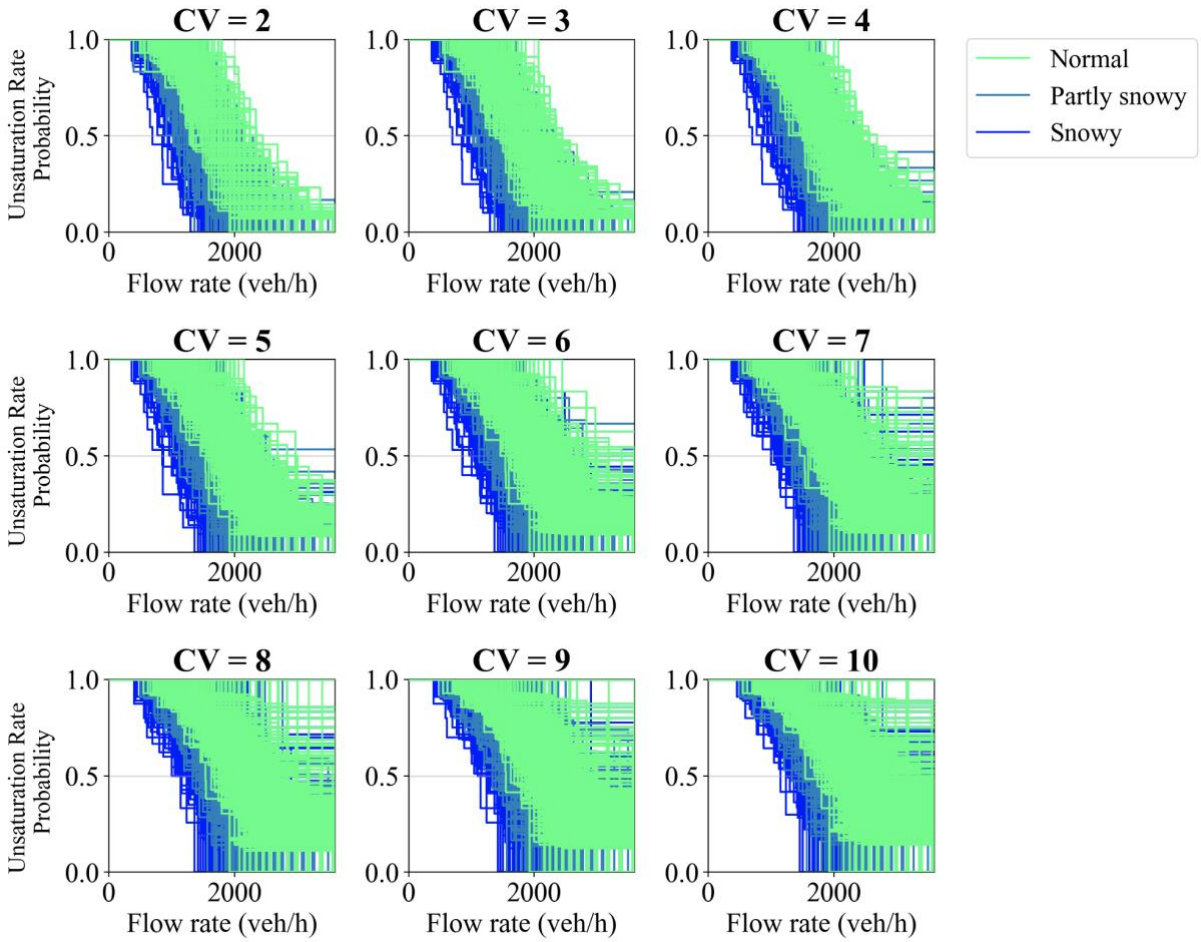

Figure 3.5: Survival Functions for Cycle-based Data

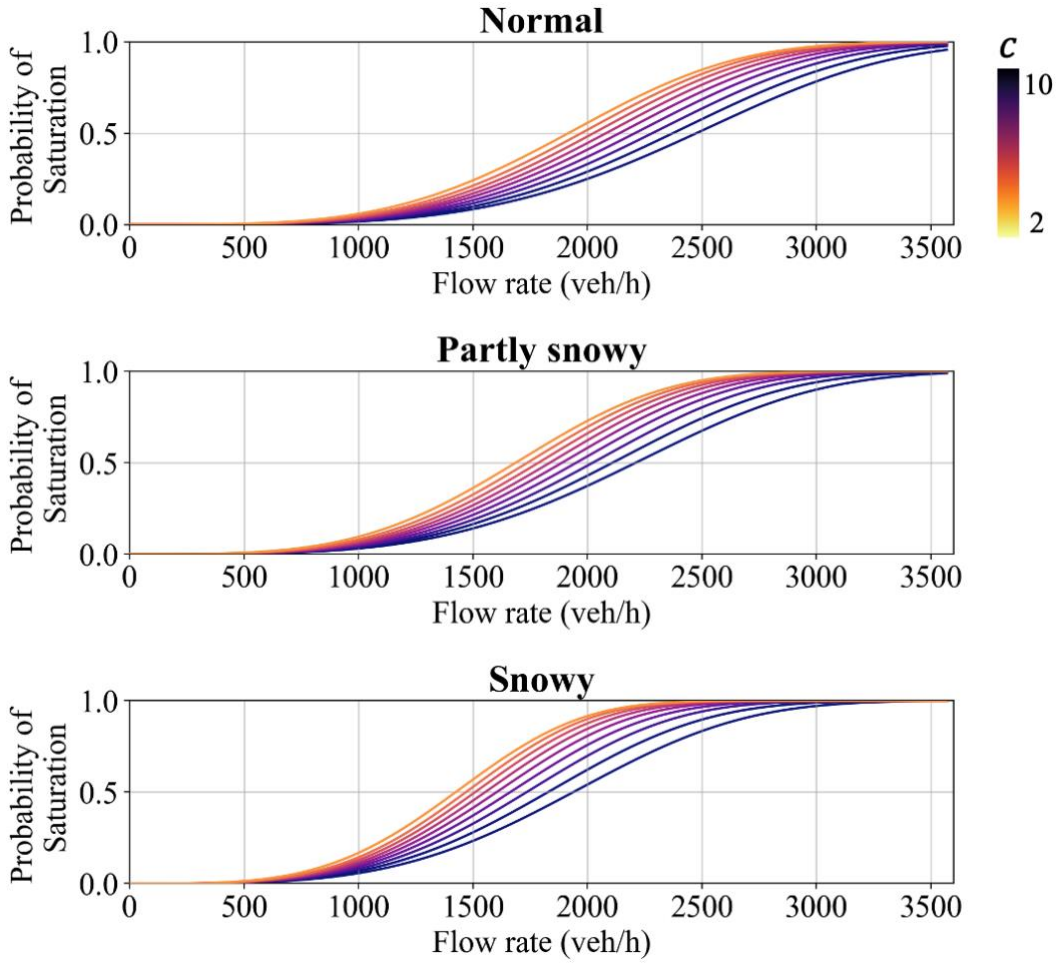

Figure 3.6: Stochastically-derived SFR Distribution

Table 3.2 Parameters of Weibull Fitting

		Critical Vehicle								
		2	3	4	5	6	7	8	9	10
Normal	λ	2113.816	2168.822	2223.142	2280.623	2343.115	2414.728	2496.585	2593.546	2706.743
	ρ	3.745	3.883	3.960	4.012	4.042	4.090	4.112	4.134	4.117
	AIC [×10^4]	19.860	18.378	16.942	15.521	14.114	12.668	11.225	9.761	8.373
Partly snowy	λ	1862.199	1912.336	1961.779	2014.031	2071.546	2138.142	2217.280	2314.383	2428.097
	ρ	3.717	3.846	3.923	3.973	3.992	4.018	4.021	3.975	3.929
	AIC [×10^4]	9.251	8.539	7.857	7.186	6.516	5.830	5.129	4.430	3.771
Snowy	λ	1570.884	1614.683	1657.647	1705.433	1761.008	1827.951	1908.176	2013.780	2138.139
	ρ	3.755	3.893	3.920	3.932	3.914	3.877	3.845	3.786	3.741
	AIC [×10^4]	5.000	4.597	4.209	3.821	3.426	3.023	2.621	2.204	1.821

3.5.2 Comparing the Performance of Stochastic and Deterministic Functions for SFR Analysis

This section compares stochastically derived distribution functions with deterministic ones under specific RW conditions and consideration of different vehicle positions as CV. Figure 3.7 provides the comparison of each pair with CVs of 2, 4, 6, 8, and 10 as examples. The probability of saturation seems to be reduced when the unsaturated vehicles in the front part of a queue are included in the distribution by the stochastic approach. This reduction is more considerable for the larger CV setting and more adverse RW conditions, i.e., the larger CV indicates that more vehicles are considered as unsaturated while snowy RW conditions amplify the effect per additional unsaturated vehicle considered.

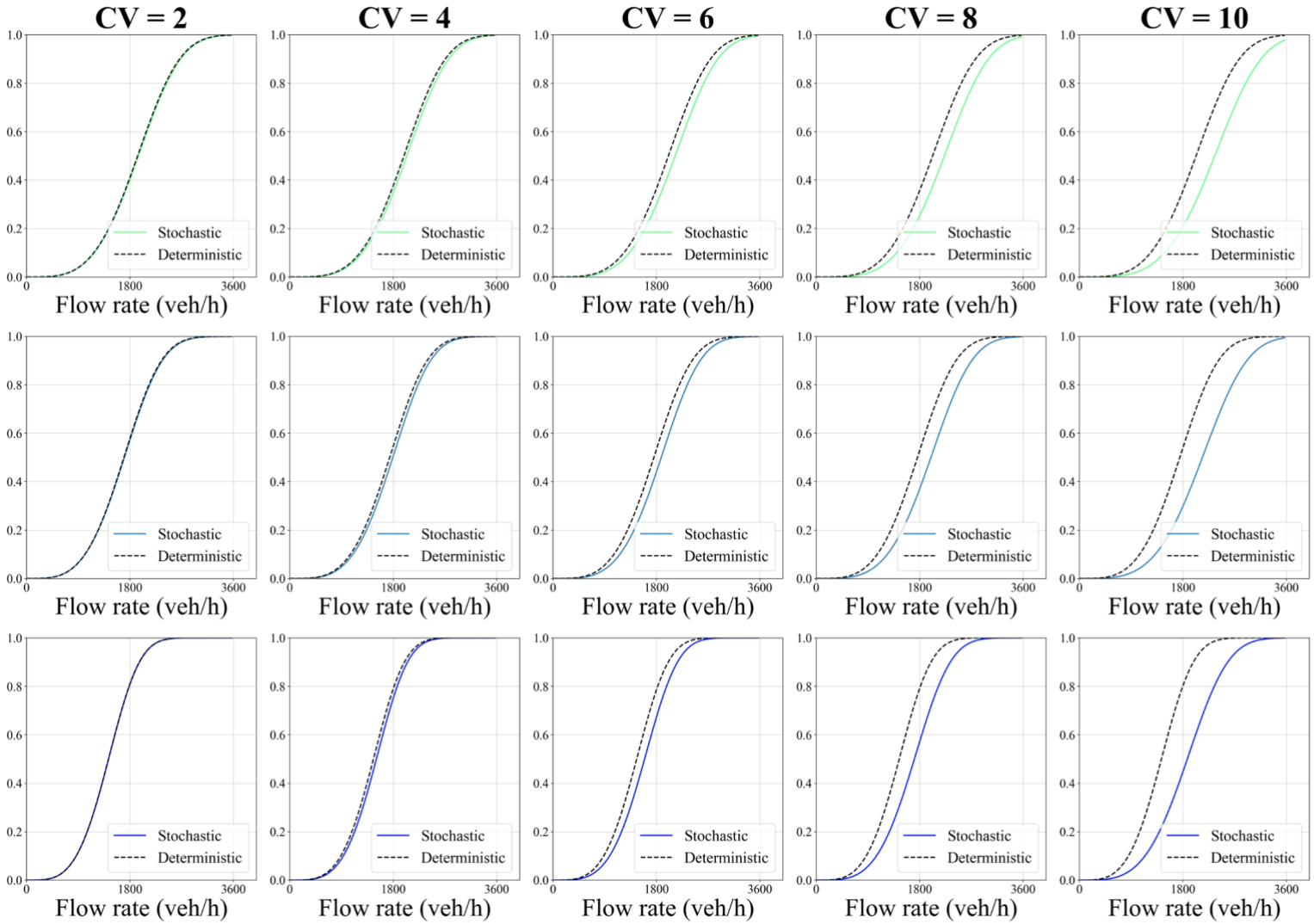

Figure 3.7: Stochastic vs Deterministic Distribution Functions

3.5.3 Determining the Optimal Critical Vehicle Threshold for SFR Analysis

A statistical analysis was conducted to: simplify SFR estimation, investigate the influence of RW conditions, and identify the optimal CV threshold. Two alternative approaches were adopted: deterministic distribution curves, and stochastic distribution curves. Adopting two distinct approaches is to allow comparing the estimated optimal CV threshold and ensures the general applicability of the proposed methods.

First, deterministic distribution curves were evaluated to find the optimal CV threshold, as presented in Figure 3.4. All pairs of distribution curves in Figure 3.4 were statistically compared using Dwass-steel pairwise comparison tests (Steel et al., 1960). The test was based on the null hypothesis H_0 and the alternative hypothesis H_1 shown below; the numbers in the cells on the heat maps in Figure 2.8 show the p-values.

H_0: The two samples are derived from the same distribution

H_1: The two samples are not derived from the same distribution

Starting from the distribution curve for CV=2, pairwise comparisons were conducted with other distribution curves (i.e., CV=3, 4…, 10) in ascending order to check if each pair of curves are significantly different. The results were visualized in the heat maps in Figure 3.8 based on the p-value of 0.05. The coloured cells i.e., the p-values greater than 0.05, indicate that the null hypothesis could not be rejected with confidence level of 95% i.e., distribution curves are not different significantly. We hypothesize that the optimal CV threshold is associated with a curve that is not significantly different from most of the other curves i.e., the curve with the highest number of insignificant p-values in a row in Figure 3.8. Thus, optimal CV thresholds for Normal, Partly snowy and Snowy RW conditions are identified by the 6^{th}, 4^{th}, and 2^{nd} vehicles in the queue, respectively. These results indicate that the position of the optimum CV moves forward to the head of the queue (i.e., lower CV values) as RW conditions deteriorate. Further, the findings clearly underline the need for recommending different optimum CVs under different RW conditions.

Second, we evaluated stochastic distribution curves to determine the optimal CV threshold under different RW conditions. The shape parameters of the Weibull distribution functions presented in Table 3.2 were investigated for combinations of RW conditions and CV thresholds. Figure 3.9 shows the variations of the shape parameter ρ as a function of different CV thresholds

for each RW condition. The shape parameter represents the failure rate in the Weibull distribution. The shape parameters in all the models in Table 3.2 are greater than 1 indicating that the failure rate increases by observed flow rate i.e., there's a higher probability of observing SFR as flow rate increases. Thus, we hypothesize that the optimum CV threshold is associated with the Weibull model which has the greatest shape parameter i.e., maximizing the probability of observing SFR as flow rate increases. Accordingly, it can be concluded that the optimal CV thresholds for Normal, Partly snowy and Snowy RW conditions are the 9^{th}, 8^{th} and 5^{th} vehicles in the queue, respectively. The findings of stochastic analysis also support the notion of using a lower CV threshold for Partly snowy and Snowy RW conditions.

Table 3.3 summarizes the findings regarding the position of the optimal CV in the queue for different RW conditions obtained through deterministic and stochastic analysis. It can be seen that the stochastic approach suggests moving the CV position to the back of a queue by three to four vehicles regardless of RW conditions. The results reveal that implementing the traditional deterministic method overestimates the probability of saturation at a given flow rate. On the other hand, the stochastic approach results in more reliable and realistic measurement of SFR by: i) suggesting to move the position of the CV to the back of the queue, thus limiting the impact of initial vehicles with longer headways in the head of the queue, ii) incorporating the data provided by unsaturated vehicle i.e., censored data, and iii) producing the distribution of SFR rather than a single deterministic value.

Table 3.3: Estimated Optimal Critical Vehicles

Approach	Normal	Partly Snowy	Snowy
Deterministic	6^{th}	4^{th}	2^{nd}
Stochastic	9^{th}	8^{th}	5^{th}

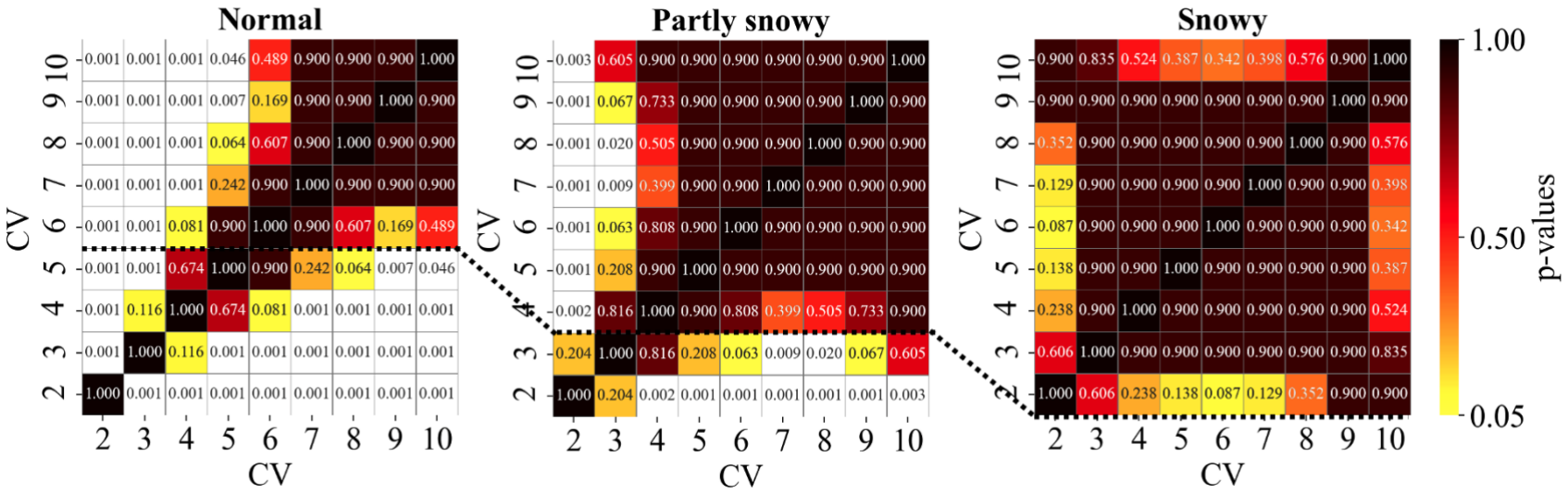

Figure 3.8: Results of All Pairwise Comparison Test

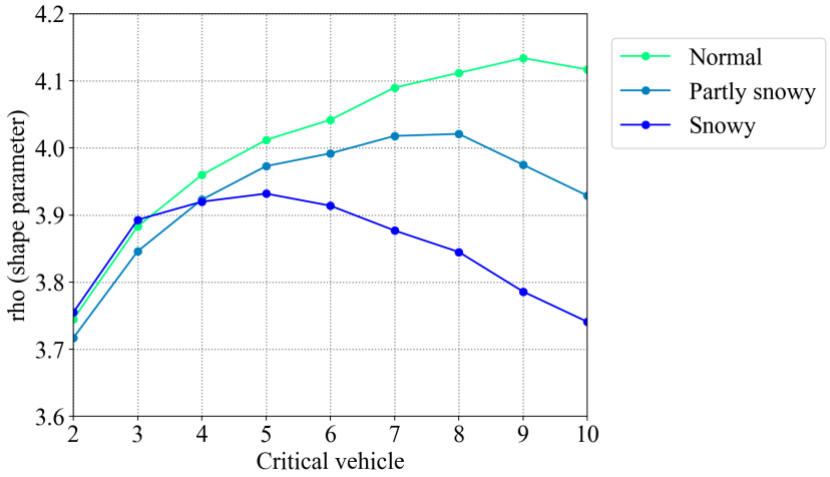

Figure 3.9: Variations of the shape parameter in fitted Weibull distributions

3.5.4 Different Distributions between Vehicle Types

In the final stage of the analysis, the impact of vehicle type on SFR variations was investigated by comparing SFR distribution functions derived through the proposed stochastic approach. Figure 3.10 presents SFR distribution functions considering different RW conditions and CV settings modelled using the headway data of PCs and HVs separately. A SFR distribution curve for HVs represents the distribution of SFR for a queue formed by HVs exclusively. It is evident from Figure 3.10 that the estimated SFR for HVs exclusively is substantially lower in comparison to PCs. Yet, the differences between the distribution curves for PCs and HVs become less significant as RW conditions deteriorate i.e., implying that HVs are less sensitive to adverse RW conditions. These observations are consistent with the findings in Hirose et al. (2022).

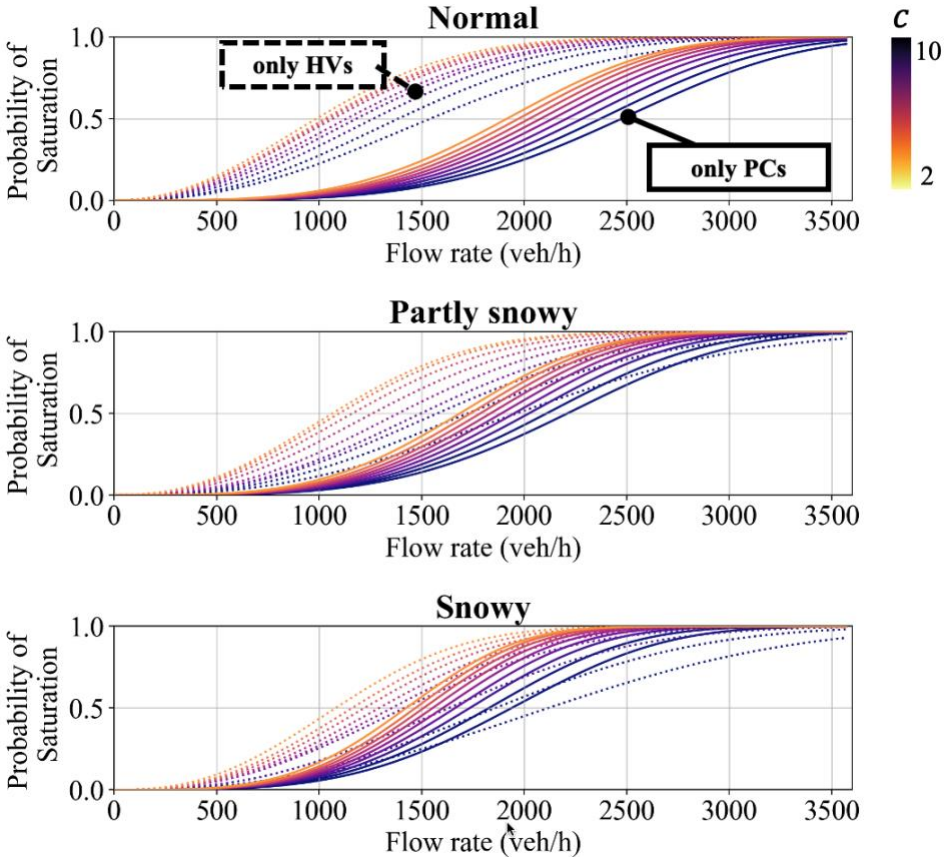

Figure 3.10: Stochastically-derived SFR Distribution of Only-HV and Only-PCs

3.6 Conclusions

This study is motivated by the lack of research on SFR analysis in cold regions aiming to: uncover stochastic characteristics of SFR, investigate the impact of RW conditions and vehicle type on SFR variations, and develop a dynamic CV threshold to improve the accuracy of SFR estimation procedure by considering its underlying stochasticity. The analysis approach adopted in this paper to fulfill these objectives consisted of three key parts. The first was to conduct survival analysis to investigate stochastic variations of SFR considering different CV thresholds and quantifying the impact of adverse RW conditions. Stochastic distribution functions of SFR estimated in this study helped to quantify how SFR decreases as snowy conditions become more intense and how such changes depend on the CV threshold considered in the analysis. Secondly, the analysis compared the performance of SFR distribution functions derived stochastically and deterministically under specific RW conditions and CV thresholds. The comparison revealed that the probability of observing saturation flow reduces significantly (especially in the case of larger CV thresholds) when the unsaturated vehicles in the front part of a queue are included in the distribution by the stochastic approach. Finally, the analysis investigated the optimal CV threshold for SFR analysis and how it varies depending on the adverse RW conditions and vehicle types. Following are the specific conclusions obtained as a result of the aforementioned analyses:

1. Snowy RW conditions decrease SFR significantly due to more conservative driving behaviour.
2. Since observed headways show a declining trend with vehicle positions in a queue before stabilizing, SFR increases significantly as CV threshold is moved toward the back of a queue.
3. When considering the unsaturated vehicles presented in the front part of the queue by the proposed stochastic approach to estimate SFR, the probability of observing saturated flow state will reduce at a given flow rate. Besides, the reduction is more considerable for larger CV settings (CV moves toward the back of the queue) and the deteriorating adverse RW conditions because the larger CV results in the inclusion of more vehicles as unsaturated and snowy RW conditions augment the effect per unsaturated vehicle considered.

4. Statistical approaches were proposed to determine an optimal position for CV based on both deterministic and stochastic SFR distribution curves. According to deterministic distribution curves, optimal CV should be 6^{th}, 4^{th} and 2^{nd} vehicle in the queue under Normal, Partly snowy and Snowy conditions. However, stochastic distribution curves indicate that the 9^{th}, 8^{th} and 5^{th} vehicles in the queue should be considered as optimum CV for each RW condition, respectively. The findings indicate that adverse RW conditions move the position of optimal CV to the front of the queue. The stochastic approach suggests moving the position of the CV to the back of the queue by three to four vehicles regardless of RW conditions.
5. HVs reduce SFR significantly. However, the impact is less pronounced under adverse RW conditions, which suggests that HVs are less prone to adverse RW conditions.

Overall, the stochastic concept of SFR by implementing the survival analysis seems to provide more realistic SFR distribution curves than the conventional deterministic calculation of SFR. Therefore, the findings of this study are expected to be helpful for practical estimation of SFR distributions at signalized intersections, as well as for investigating SFR variations under adverse RW conditions. Furthermore, this paper proposed a flexible approach to determine the optimal CV, which could simplify SFR estimation considering different RW conditions.

Lastly, as with any research, this study has limitations, which motivates several future research extensions. For example, this study did not consider the effect of clearance lost time of the last part of a queue due to data limitations, although those vehicles could also be considered as a part of the unsaturated flow (censored data). Besides, large-scale data collection efforts are required to quantify the suggested benefits of using the proposed stochastic approach. It is also recommended to verify the recommended CV thresholds for SFR calculation using empirical studies. Finally, the method to specify the optimal CV can be expanded to allow considerations for different local conditions, driver population, and traffic composition.

4 CONCLUSIONS AND RECOMMENDATIONS

4.1 Conclusions

Adverse road-weather (RW) conditions are typical temporal bottlenecks resulting in capacity drop at signalized intersections . Traffic authorities in cold areas try to implement weather-responsive traffic management (WRTM) schemes which are designed to mitigate undesirable weather-related consequences. The strategies, however, are not widely used in practice due to the limited number of supporting studies and the need for local investigations. There is also technological limitations at play, e.g., a difficulty in testing high-resolution predictions of road weather. It is an inevitable task to further study weather-related impacts on the traffic performance of signalized intersections in winter. In addition, for the recent importance of reliability of transportation systems represented by demand responsive traffic control, traffic management that adapts to adverse weather and traffic conditions is expected to become increasingly important (Gorev et al., 2020). Therefore, filling the research gaps is now a key to establishing future intelligent transportation systems.

This thesis statistically analyzed the negative effects of adverse RW conditions on saturated traffic at signalized intersections using the data collected in Winnipeg, Canada. The focus of this thesis was to show the combined impact of adverse RW and heavy vehicles (HVs) on saturation headways. This thesis also proposed a novel stochastic analysis approach to estimate saturation flow rate (SFR) by considering the additional censored data provided by unsaturated vehicles in the queuing traffic.

4.1.1 Influence of adverse RW on saturated traffic

Throughout this thesis, it was aimed to clarify the influence of adverse RW conditions on saturation headway. Overall, the results confirmed that adverse RW conditions significantly increased saturation headway at signalized intersections while the difference by lane was found insignificant. Besides, further analysis of the impact of adverse RW conditions suggest deploying variable optimal critical vehicle (CV), where SFR becomes stabilized, by moving the CV forward in a discharging queue as RW conditions deteriorates. The proposed analysis method and results will support traffic managers in deciding on the implementation of WRTM, specifically in cold regions with comparable RW conditions with Winnipeg, Manitoba and provides easy to use and practical

adjustment factors for SFR to account for the impact of adverse RW conditions. Provision of SFR adjustment factors per lane coupled with determination of optimal CV position under adverse RW conditions enables reliable and accurate analysis of SFR considering different RW conditions, which contribute to establishment of efficient WRTM schemes in cold regions.

Among the major findings on this topic were:

- Saturation headways under Partly snowy and Snowy were 13.6% and 38 % longer than Normal, respectively. The multiple regression model developed also showed Snowy RW conditions had the most significant effect on the increase in saturation headway among the variables analyzed (Chapter 2).
- The mean saturation headway on the median lane was 5% shorter than that of the center lane. However, the difference in saturation headways across the lanes was not statistically significant in adverse RW conditions (Chapter 2).
- The position of the optimal CV, at which the flow rate begins to stabilize as SFR, moves forward in the queue for adverse RW conditions (Chapter 3).

4.1.2 HV's interference with SFR under adverse RW

Next, this study added the HV's interference on the effect of adverse RW conditions on saturation headway. The results from estimated passenger car equivalent (PCE), the regression model, and SFR distribution curves, consistently indicated that HVs were less sensitive to adverse RW conditions than passenger cars (PCs) in terms of their impact on SFR. Yet, observed inconsistencies between HV and PC driver behaviours pose additional risks to road users under adverse RW conditions. Based on this observation, implementation of WRTM at signalized intersections should be focused on harmonizing the driving behaviour in terms of turning and lane changing maneuvers, driving speed, and following behaviour. Application of dynamic lane operations such as exclusive HV lanes under adverse RW conditions for intersections with high HV % could be explored further as a viable option.

Among the major findings on this topic were:

- The presence of HVs under adverse RW conditions was found to significantly increase the saturation headway of each cycle (Chapter 2).
- The measured relative PCE values compared the impact of HVs and PCs under the same RW conditions on traffic. PCE under Normal RW conditions was 2.07, while it was 1.72 for Partly snowy and 1.47 for Snowy. According to model coefficients estimated for HV ratio through regression analysis, the impact of HV ratio on saturation headways appeared less significant as RW conditions deteriorate i.e., shifts from Normal to Snowy (Chapter 2).
- HVs reduced SFR significantly, while the effect became negligible under Snowy RW conditions (Chapter 3).

4.1.3 Proposed analytical tools

This thesis suggested some analytical tools for future investigations and studies. The analysis in Chapter 2 revealed that lognormal distribution closely reproduces saturation headway distributions. The fitted functions would enable calibration of micro-simulation models under different RW conditions. Once RW conditions, HV ratio, time of observation and geometric conditions of the signalized intersection are known, the developed regression models could be used to estimate the variations of saturation headway considering the impact of RW conditions and HVs, enabling accurate evaluation of signal settings to improve intersection performance. Moreover, the inverse function of the models could be considered to establish informed speculations regarding potential RW conditions based on observed saturation headway information. Thus, if traffic monitoring systems across a city automatically record the individual vehicle's headways at signalized intersections, traffic managers will be able to potentially comprehend which part of the city is severely affected by weather events, which is very useful for planning efficient winter maintenance operations.

Additionally, the foremost objective of this paper was to propose a stochastic concept to investigate SFR variations at signalized intersections under different RW conditions. The unsaturated vehicles, which always exist in the traffic stream in the front part of the waiting queue, are indiscriminately excluded from SFR analysis in the conventional deterministic approach. On

the other hand, the proposed reliability-based (survival analysis) approach could produce comprehensive SFR distribution functions obviating the bias. Hence, using this concept, traffic managers can determine the range of expected variations in intersection capacity to meet the desired level of service target. Besides, the availability of realistic SFR distribution functions is expected to improve the design of signal timing and reliability of transportation systems across a city. For example, once we know the precise reliability of every intersection along a corridor, it is beneficial to understand the reliability of the corridor and even transportation system-level. Lastly, this thesis suggested statistical methodologies that would determine optimal CVs for different traffic and RW conditions. The methodological contribution is expected to enhance the efficiency of potential WRTM schemes for signalized intersections.

Among the major findings on this topic were:

- Saturation headway distributions found to follow left-skewed lognormal distribution functions (Chapter 2).
- The established multiple regression model showed its significance and adequate prediction power to estimate saturation headway with respect to the HV ratio under different RW conditions (Chapter 2).
- The proposed stochastic approach exhibited the reduction in the probability of saturation happened because of unsaturated vehicles in traffic. Besides, the reduction was more considerable for the larger CV setting and the more adverse RW (Chapter 3).
- The proposed method to determine an optimal CV threshold would be beneficial in finding localized CV under different combinations of RW conditions and HV ratio (Chapter 3).

4.2 Recommendations

The research conducted in this thesis has its limitations as per several simplifying assumptions and hypotheses to be verified and/or removed in future extension of this research. The following directions for future research are hereby identified:

- **Collecting more accurate and reliable data**

The findings on saturation headways and SFR relied on the manually collected headway data using a video processing software, while RW conditions were classified primarily in a visual setting. Since getting more accurate data is of paramount importance, it is advisable, for example, to use automated vehicle detection sensors along with Road Weather Information Systems to expand the research. Thusly collected data will be more reliable, representative and away from human-oriented error; what is more, it will help secure a large sample size.

- **Improving model accuracy**

The established regression model in Chapter 2 demonstrated adequate explanatory power for estimation of saturation headways with 95 % significance and reasonably low MAPE. However, considering the lower R-squared values, the model should be further improved by examining non-linear models and consideration of other influential explanatory variables.

- **Testing geographical stability**

This research studied two specific signalized intersections in Winnipeg, Manitoba. Investigating the applicability of the proposed models to other locations is vital for establishing universal and generalized methods. For this purpose, the models should be calibrated using the data collected in additional locations with comparable RW conditions, and the estimated outputs should be compared with the actual observations.

- **Investigating the effect of the reduced traffic demand under inclement weather**

Adverse RW changes not only the driving behaviour but also the individual travel patterns. Due to the reduced traffic demand in inclement weather (Maze, 2005), the benefit of using WRTM with the proposed methods could be less significant. Cost-benefit analysis of the implementation of WRTM under the reduced traffic should be conducted.

- **Considering clearance lost time to SFR**

Clearance lost time is also a concern that could be affected by adverse RW conditions. In future research investigating the impacts of adverse RW conditions, the unsaturated flow rates with

clearance lost time should be included into the stochastic concept of SFR distributions, and the impact on the distributions should be investigated further.

- **Evaluating the actual benefit of the stochastic concept**

This thesis did not assess the tangible benefit of incorporating the stochastic concept into adaptive signal timing design. Comparing the capacity, delay and fuel consumption before and after the implementation would justify using the stochastic concept. For this purpose, it is recommended to conduct a comparative study using simulation or field observations.

References

Agbolosu-Amison, S. J., Sadek, A. W., & EiDessouki, W. (2004). Inclement weather and traffic flow at signalized intersections: Case study from Northern New England. *Transportation Research Record*, *1867*, 163–171. https://doi.org/10.3141/1867-19

Alhassan, H. M., & Ben-edigbe, J. (2012). Evaluation of Passenger Car Equivalent Values Under Rainfall. *International Conference On Traffic And Transportation Engineering*, *26*(Ictte), 6–10. http://www.ipcsit.com/vol26/2-ICTTE2012-T005.pdf

Asamer, J., & Van Zuylen, H. J. (2011). Saturation flow under adverse weather conditions. *Transportation Research Record*, *2258*, 103–109. https://doi.org/10.3141/2258-13

Balke, K. N., Chaudhary, N., Sunkari, S., Charara, H., Florence, D., Stevens, C., Pesti, G., & Tydlacka, J. (2017). *Guidelines for Deploying Weather Responsive Operations in TxDOT Traffic Signals*.

Botha, B. J. L., Kruse, T. R., & Member, S. (1992). Flow Rates at Signalized Intersections under Cold Winter Conditions. *The Journal of Transportation Engineering*, *118*(3), 439–450.

Brilon, W., Geistefeldt, J., & Regler, M. (2005). Reliability of Freeway Traffic Flow. *Transportation and Traffic Theory*, *July*, 125–144. https://doi.org/10.1016/b978-008044680-6/50009-x

ITE (The Institute of Transportation Engineers) (2007). Canadian Capacity Guide for Signalized Intersections 3rd edition.

City of Winnipeg, 2019. 2019 Traffic Flow Map: Average Weekday Daily Traffic on Major Streets. Retrieved from https://winnipeg.ca/publicworks/trafficControl/trafficData/trafficFlowMap.stm.

Chaudhry, M. (2013). *Capacity Analysis of Signalised Intersections: Effects of Green Time on Saturation Flow Rate* (Vol. 1994). The University of Auckland.

Chauhan, R., Dhamaniya, A., Arkatkar, S., Sahu, P., Vikram, D. (2019). Effect of Side Friction Parameter on Urban Road Traffic: Under Mixed Traffic Scenario. *Journal of the Eastern Asia Society for Transportation Studies*, *13*, 314–330. https://doi.org/10.11175/easts.13.314

Chodur, J., Ostrowski, K., & Tracz, M. (2011). Impact of saturation flow changes on performance of traffic lanes at signalised intersections. *Procedia - Social and Behavioral Sciences*, *16*, 600–611. https://doi.org/10.1016/j.sbspro.2011.04.480

Gorev, A., Popova, O., & Solodkij, A. (2020). Demand-responsive transit systems in areas with low transport demand of "smart city." *Transportation Research Procedia*, *50*(2019), 160–166. https://doi.org/10.1016/j.trpro.2020.10.020

FHWA (The Federal Highway Administration). (n.d.). *Corridor Simulation (CORSIM/TSIS)*. Retrieved July 18, from https://ops.fhwa.dot.gov/trafficanalysistools/corsim.htm

FHWA (The Federal Highway Administration) (2017). *Weather Responsive Management Strategies (WRMS)– Minnesota DOT Case Study*. Retrieved from https://ops.fhwa.dot.gov/publications/fhwahop19080/fhwahop19080.pdf

FHWA (The Federal Highway Administration) (2001). Traffic Monitoring Guide. U.S. Department ofTransportation, Washington, D.C..

FHWA (The Federal Highway Administration) (n.d.). *Weather-Responsive Management Strategies*. Retrieved from http://www.ops.fhwa.dot.gov/weather

TRB (Transportation Research Board) (1985). Highway Capacity Manual 3rd. Washington, D.C..

TRB (Transportation Research Board) (2000). Highway Capacity Manual 4th. Washington, D.C..

TRB (Transportation Research Board) (2010). Highway Capacity Manual 5th. Washington, D.C..

TRB (Transportation Research Board) (2016). Highway Capacity Manual 6th. Washington, D.C..

Hirose, R., Mehran, B., & Pani, A. (2022). Investigating Combined Impact of Adverse Road-Weather Conditions and Heavy Vehicles on Saturation Headway. *Transportation Research Record*. https://doi.org/10.1177/03611981221089303

Historical Climate Data. Government of Canada. Retrieved March 1st, 2021, from https://climate.weather.gc.ca/historical_data/search_historic_data_e.html

Ibrahim, A. T., & Hall, F. L. (1994). Effect of adverse weather conditions on speed-flow-occupancy relationships. *Transportation Research Record*, *1457*, 184–191.

Kaplan, E. L., & Meier, P. (1958). Nonparametric estimation from incomplete samples. *Journal of the American Statistical Association*, *53*(282), 457–481. http://www.jstor.org/stable/2281868

LaVela, S. L., Evans, C. T., Miskevics, S., Parada, J. P., Priebe, M., & Weaver, F. M. (2007). Long-term outcomes from nosocomial infections in persons with spinal cord injuries and disorders. *American Journal of Infection Control*, *35*(6), 393–400. https://doi.org/10.1016/j.ajic.2006.08.012

Lu, Z., Kwon, T. J., & Fu, L. (2019). Effects of winter weather on traffic operations and optimization of signalized intersections. *Journal of Traffic and Transportation Engineering (English Edition)*, *6*(2), 196–208. https://doi.org/10.1016/j.jtte.2018.02.002

Luo, Q., Yuan, J., Chen, X., Wu, S., Qu, Z., & Tang, J. (2019). Analyzing start-up time headway distribution characteristics at signalized intersections. *Physica A: Statistical Mechanics and Its Applications*, *535*, 122348. https://doi.org/10.1016/j.physa.2019.122348

Manitoba Public Insurance (MPI). (2020). *Manitoba public insurance 2020 traffic collision statistics report*.

Maze, T. H., Agarwal, M., & Burchett, G. (2005). *Whether Wheather Matters To Traffic Demand* (Issue August).

McTrans. (2021). *TRANSYT-7FTM - Traffic Network Study Tool - User guide*.

NTOC, 2012. 2012 National traffic signal report card: technical report. Retrieved from http://library.ite.org/pub/e265477a-2354-d714-5147-870dfac0e294.

Pisano, P. A., & Goodwin, L. C. (2004). Research Needs for Weather-responsive Traffic management. *Journal of the Transportation Research Board*, *1867*, 127–131. https://doi.org/10.1007/978-3-319-78262-1_300662

Perrin, J., Martin, P. T., & Hansen, B. G. (2001). Modifying Signal Timing During Inclement Weather. *Transportation Research Board 80th Annual Meeting January 7-11, 2001 Washington, D.C., No. 01-3233*.

Prevedouros, P. D., & Chang, K. (2005). Potential effects of wet conditions on signalized intersection LOS. *Journal of Transportation Engineering*, *131*(12), 898–903. https://doi.org/10.1061/(ASCE)0733-947X(2005)131:12(898)

Sadek, A. W., & Amison-Agbolosu, S. J. (2004). *Validating Traffic Simulation Models to Inclement Weather Travel Conditions with Applications to Arterial Coordinated Signal Systems*. *March*.

Schoenfelder, S., & Axhausen, K. W. (2000). *Analysing the rhythms of travel using survival analysis* (Issue July). https://doi.org/https://doi.org/10.3929/ethz-a-004241369

Steel, R. G. D (1960). A Rank Sum Test for Comparing All Pairs of Treatments. Technometrics, Vol. 2, No. 2, pp. 197–207.

Suzuki, K., & Nakamura, H. (2016). TrafficAnalyzer - The Integrated Video Image Processing System for Traffic Flow Analysis. Proceedings of the 13th World Congress on Intelligent Transportation Systems, London.

Trafficware, Ltd. (2011). *Synchro Studio 8 Traffic Signal Software-User Guide.* Sugar Land, TX: Trafficware, Ltd.

Teply, S. (1977). A Canadian Problem – Winter Intersection Capacity.. Proceedings of Technical Papers, Annual Conference of the Institute of Transportation Engineers, District 7, Canada, Vol.2, 39-50.

Teply, S. (1983). Saturation flow at signalized intersection through magnifying glass. In Proc., Eighth International Symposium on Transportation and Traffic Flow Theory. Toronto University Press.

Webster, F.V. & Cobbe, B.M. (1966). Traffic Signals. *Road Research Technical Paper*, No. 56, Road Research Laboratory, Her Majesty Stationary Office, London, U.K.

Yasanthi, R. G. N., & Mehran, B. (2020). Modeling free-flow speed variations under adverse road-weather conditions: Case of cold region highways. *Case Studies on Transport Policy*, *8*(1), 22–30. https://doi.org/10.1016/j.cstp.2020.01.003

Appendix

Example of Dataset for Headways at Century intersection

Year	Month	Day	Date	RW class	RW class2	Timezone	Temparature	Time	Cycle ID	ID	Headway	Vehicle
2020	Jan	9	Thu	6	2	AM	-12.3	7:32:26	1	1	0	PC
2020	Jan	9	Thu	6	2	AM	-12.3	7:32:29	1	2	2.95	PC
2020	Jan	9	Thu	6	2	AM	-12.3	7:32:32	1	3	2.85	PC
2020	Jan	9	Thu	6	2	AM	-12.3	7:32:34	1	4	2.4	PC
2020	Jan	9	Thu	6	2	AM	-12.3	7:32:36	1	5	1.95	PC
2020	Jan	9	Thu	6	2	AM	-12.3	7:32:39	1	6	2.45	PC
2020	Jan	9	Thu	6	2	AM	-12.3	7:32:42	1	7	2.9	PC
2020	Jan	9	Thu	6	2	AM	-12.3	7:32:44	1	8	2	PC
2020	Jan	9	Thu	6	2	AM	-12.3	7:32:45	1	9	1.4	PC
2020	Jan	9	Thu	6	2	AM	-12.3	7:32:48	1	10	2.8	PC
2020	Jan	9	Thu	6	2	AM	-12.3	7:32:50	1	11	2.45	PC
2020	Jan	9	Thu	6	2	AM	-12.3	7:32:53	1	12	2.35	PC
2020	Jan	9	Thu	6	2	AM	-12.3	7:32:54	1	13	1.6	PC
2020	Jan	9	Thu	6	2	AM	-12.3	7:32:57	1	14	3.1	PC
2020	Jan	9	Thu	6	2	AM	-12.3	7:34:55	2	1	0	PC
2020	Jan	9	Thu	6	2	AM	-12.3	7:34:58	2	2	3.05	PC
2020	Jan	9	Thu	6	2	AM	-12.3	7:35:01	2	3	2.45	PC
2020	Jan	9	Thu	6	2	AM	-12.3	7:35:05	2	4	4.45	AV
2020	Jan	9	Thu	6	2	AM	-12.3	7:35:09	2	5	3.95	PC
2020	Jan	9	Thu	6	2	AM	-12.3	7:35:12	2	6	2.4	PC
2020	Jan	9	Thu	6	2	AM	-12.3	7:35:13	2	7	1.7	PC
2020	Jan	9	Thu	6	2	AM	-12.3	7:35:17	2	8	3.8	PC
2020	Jan	9	Thu	6	2	AM	-12.3	7:35:19	2	9	2.4	PC

NOTE:
[1] RW class is ID for the initial 7 RW classifications
[2] RW class2 is ID for 3 types of combined RW classifications
[3] ID is the position of the vehicle in a queue per cycle